Journal of
Composites Science

MDPI

Article

An Optimal Selection of the Clamping Fixture for Manufacturing an I-Shaped Composite Beam

Ju Qiu [1,2], Chundu Sun [1], Huaxiang Rao [1], Youhong Gong [1] and Jiali Tang [1,*]

[1] COMAC Shanghai Aircraft Manufacturing Co., Ltd., Composites Center, Shanghai 200123, China; qiu_x_j@126.com (J.Q.)
[2] Beijing Key Laboratory of Civil Aircraft Structures and Composite Materials, COMAC Beijing Aircraft Technology Research Institute, Beijing 102211, China
* Correspondence: tangjiali@comac.cc

Abstract: In this paper, the influence of the different clamping zones of a web on the vibration of I-shaped composite beams is discussed. This current study is divided into two steps. In the first step, according to the different clamping spacings, through vibration simulation analysis, the optimal clamping spacing was selected. In the second step, the optimal new fixture was designed by means of different clamping positions and shapes. The analysis also reveals that a reduction in the clamping space does not contribute to a reduction in vibration. A newly selected fixture was designed based on the results that were delivered by the finite element model analysis of the L fixture in the upper and lower. Based on static analysis, the improved fixture was able to significantly reduce displacement, stress, and strain compared with the original one. By using dynamic analysis, modes, the frequency response, and random analyses, we found that the improved fixture could enhance the natural frequencies of the structure and reduce vibration displacement and acceleration during manufacturing. From the 2000 Hz sweep, the peak values of the power spectral density of displacement and acceleration went down by about 100 and 10 times, respectively.

Keywords: I-shaped composite beam; fixture; mode analysis; vibration analysis; random vibration analysis

Citation: Qiu, J.; Sun, C.; Rao, H.; Gong, Y.; Tang, J. An Optimal Selection of the Clamping Fixture for Manufacturing an I-Shaped Composite Beam. *J. Compos. Sci.* **2023**, *7*, 369. https://doi.org/10.3390/jcs7090369

Academic Editor: Francesco Tornabene

Received: 20 August 2023
Accepted: 29 August 2023
Published: 4 September 2023

1. Introduction

Manufacturing is the major pillar of the national economy and occupies an important position in the economic growth of both developed and developing countries. With increasing market competition and increasing attention to social and environmental protection issues, governments, enterprises, and users around the world prioritize high-efficiency, eco-friendly, and low-cost manufacturing.

Composite thin-walled parts have been widely used in many fields due to their advantages, such as lightweight, high specific strength, relatively high specific stiffness, and low machining tolerance. However, these materials are difficult to machine due to their poor rigidity and large vibration amplitude and deformation, often limiting the machining quality. Given their importance and extensive application, the vibration deformation of thin-walled composites in processing has always been a concern. There has been a lot of effort to find solutions to overcome these problems, with many ideas and solutions proposed and implemented in practice.

Under actual practice, the preparation cycle of the equipment for the process accounts for about half of the total and about 70% of the time spent during the process of fixture design, which is an element that significantly affects the design process. The fixture quality also greatly affects the product process.

In more recent years, with regard to fixture design, some studies show the use of direct static analysis in conjunction with modal analysis. Other research presents the use of optimization methods in designing fixtures, while others propose new methods including

intelligent tools for fixture design. Additionally, engineers have come forward with online health monitoring for fixtures.

Prajwal Shenoy et al. [1] investigated the behavior and analyzed a split fixture under varying static loading conditions. They considered the effect of dynamic loads on the split fixture, including auxiliary assembly components in design analysis. Olabanji Olayinka et al. [2] proposed a detailed design of the parts of the fixture. The stress and displacement analysis of the parts were performed using Solid Works to express simulation. The parameters of the hydraulic components were evaluated from force requirements, and the hydraulic system was physically modeled using MATLAB Simscape hydraulics.

Amaral N.R. et al. [3] used ANSYS parametric design language (APDL) code to develop an algorithm to automatically optimize fixture support, clamping locations, and clamping forces with the scope to minimize workpiece deformation, subsequently increasing machining accuracy. Khan A. et al. [4] used the ANSYS parametric design language optimization tool to automatically identify locator and clamp positions that yielded the minimum workpiece deformation. YanFeng Xing [5] showed that a proposed optimization algorithm suitably generated the optimal fixture layout with excellent efficiency for engineering applications. Xing Yanfeng et al. [6] proposed a new method to optimize the fixture scheme by a non-domination sorting social radiation algorithm (NSSRA). Zoppi Matteo et al. [7] concluded that the optimization procedure for the fixture layout combined with a genetic algorithm and a finite element analysis yielded good output results for the simulation in a case study.

Andrew Illidge and Glen Bright [8] proved in a selected condition that a fixture known as an automated flexible fixture system (AFFS) could be designed to meet all set requirements. Vijaya Ramnath Elanchezhian et al. [9] developed a milling fixture and its clamping setup for a vertical milling machine in which friction stir welding operations were performed. Zhipeng Liang et al. [10] proposed a novel fixture configuration scheme providing a new approach for automatic up and down machining of the long ladder shaft gear. Kuigang Yu et al. [11] proposed a design method of the flexible fixture system for specific automotive body parts, which contained a structure and locating control algorithm design of compliant fixtures. Aiming at providing an effective mechanism for the representation, organization, and reuse of fixture design knowledge, F. P. Zhang et al. [12] proposed an intelligent methodology for fixture design based on knowledge component technology.

Denkena Berend et al. [13] introduced a sensory workpiece clamping system that utilized sensory swing clamps. The device was developed in prior research work in order to provide monitoring capabilities for the cutting forces. They took up the experimental analysis of the multiple integrated sensors of the sensory swing clamp and the characterization of their measuring capability toward different measures.

The above review indicates that the fixture is the principal part of the process equipment, which is indispensable in the fabrication process. It is also in the machining process to fix parts of a process device, whose role is to ensure that parts in the processing project have the correct and accurate position. The main functions of the fixture are as follows:

1. Provide processing quality;
2. Improve productivity and reduce cost;
3. Expand the scope of machining.

According to the power source of the clamping device, a fixture can be classified as a manual fixture, pneumatic fixture, hydraulic fixture, electromagnetic fixture, etc. As the object of interest is the large-scale thin-walled composite I-shaped beam, such geometry could be easily deformed before and after processing. In order to ensure processing stability, improve productivity and reduce labor effort, the parts' holders in this paper use a pneumatic fixture. The following principles should be followed when the fixture is designed:

1. The clamping of the fixture must be stable and reliable;
2. The fixture must be of good operability;
3. The fixture must deliver sufficient holding strength and stiffness;

4. The fixture design must be reasonably economical while meeting the requirements of sufficient strength and rigidity.

Static and dynamic structural assessment by use of finite element analysis is typical in fixture design to examine the deformation and stress distribution of workpieces, fixtures or the major stressed parts of the fixture. Generally speaking, the workflow of fixture design is illustrated in Figure 1.

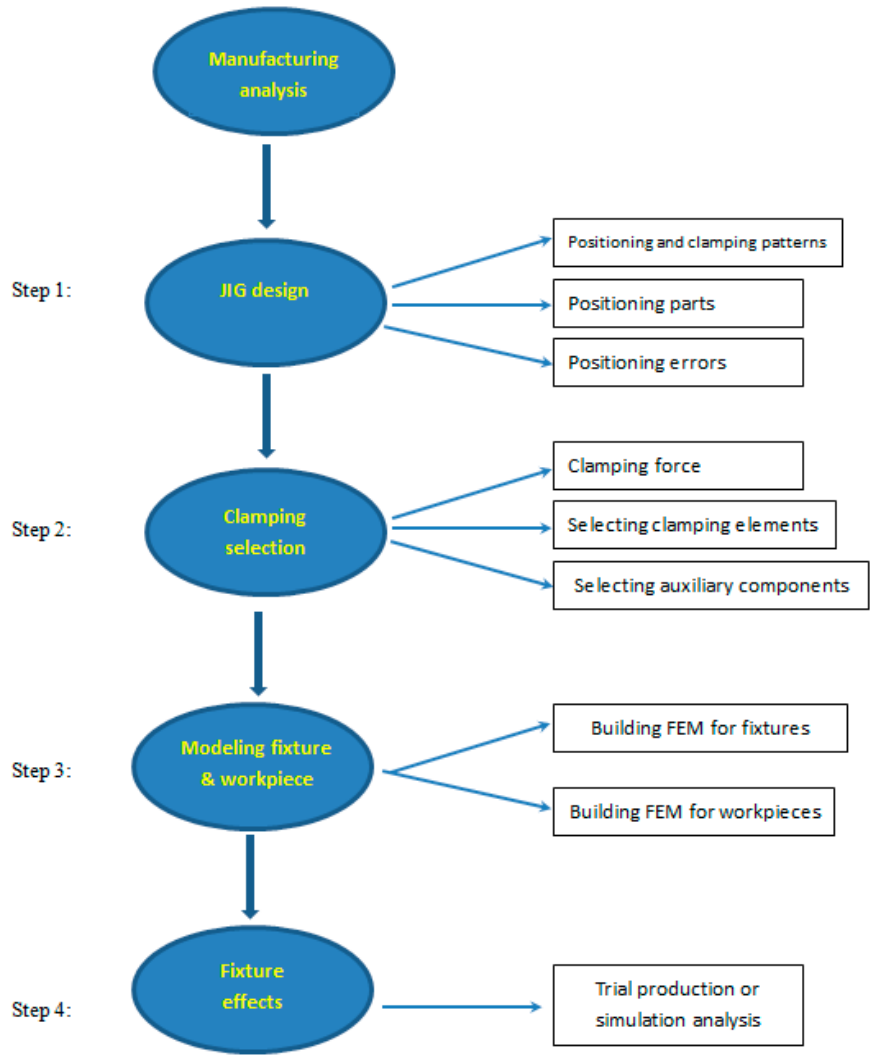

Figure 1. The flow chart of fixture design.

This paper focuses on the third and fourth steps of the exhaustive introduction. At present, in the processing of an I-shaped beam, the induced vibration is relatively large, which may cause defects in the processing parts. To improve the stiffness of the machined parts, we propose a reduction in the distance between the fixtures on the webs to increase the rigidity. Three distances, 0.2 m, 0.3 m, and 0.4 m are considered for the clamping spacing. After comparison and analysis, we optimally choose the 0.4 m clamping distance. Through the static and dynamic analysis using finite element models of the different clamping locations and modes and under actual working conditions, the natural frequency, stress, deformation, and vibration response during machining are analyzed, and the coherence of the design along with the response characteristics of the key parts are checked. This paper proposes a novel processing fixture, which changes the clamping pattern and position of the I-shaped beam but reduces its vibration and tool wear.

2. Design of the Fixture with Different Spacing

2.1. The Finite Element Model

In the finite element model, the workpiece's boundary condition and the loaded model with the discrete spacing of clamping in the machining process are established. According to the current machining scenario, the I-beam is clamped on the web as illustrated on the left side of Figure 2. The cross-sectional view of the right side is also shown in Figure 2.

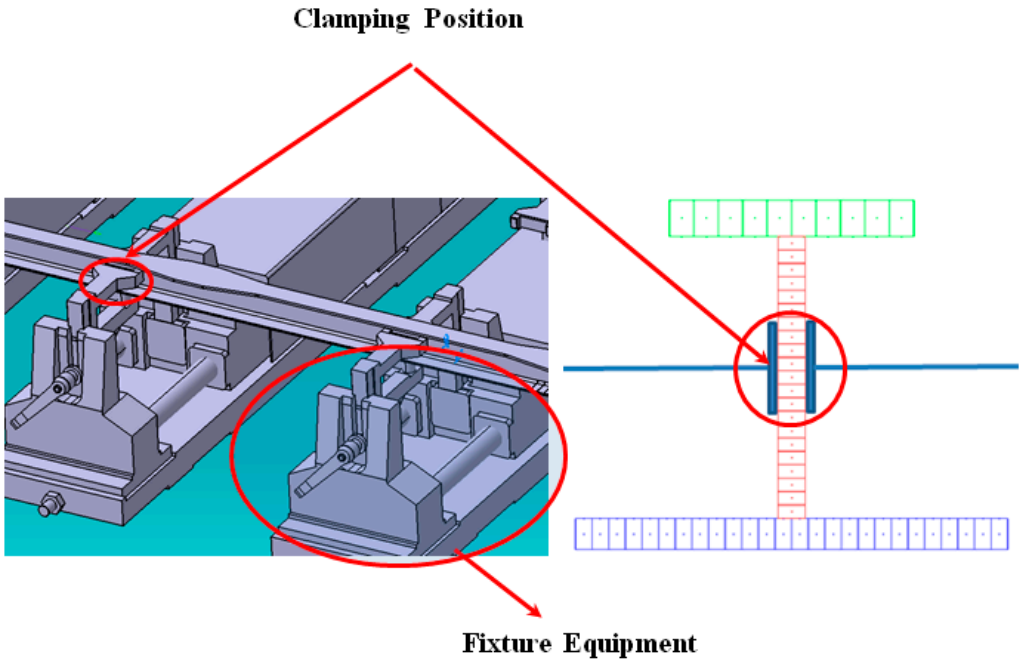

Figure 2. The illustration of the present approach in clamping on the web.

The workpiece is 1.5 m long. The clamping position is identified as a constraint of the web in the model. The meshing dimension is 2 mm X 2 mm. There are 42,750 2-D elements and 43,558 nodes. The dynamic model of the original fixture clamping spacing model (Case 1) is shown in Figure 3.

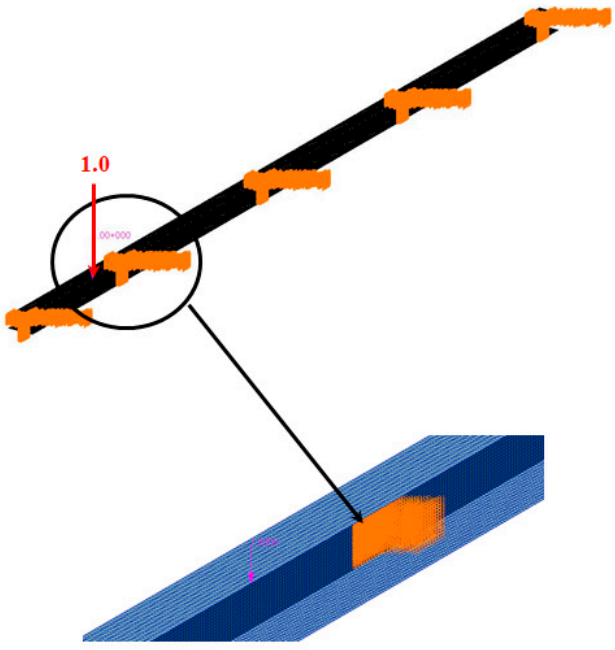

Figure 3. Clamping on the web for FEM (space between clamps: 0.4 m).

A finite element dynamic analysis model (Case 2) is established by using a reduced clamping distance of 0.3 m, as shown in Figure 4.

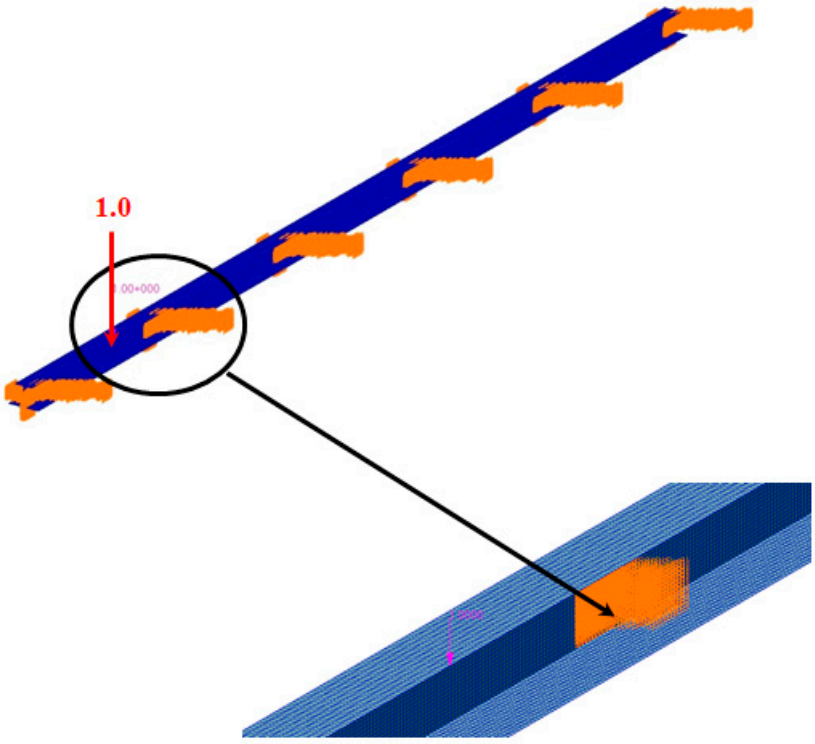

Figure 4. Clamping on the web for FEM (space: 0.3 m).

The above models' material parameters are given in Table 1.

Table 1. The material properties table.

Mechanics Properties	E_1 (GPa)	E_2 (GPa)	E_3 (GPa)	G_{12} (GPa)	G_{13} (GPa)	G_{23} (GPa)	v_{12}	v_{13}	v_{23}
Parameters	169	4.49	4.49	1.628	1.628	0.5435	0.33	0.33	0.45

Flange and web laminations are presented in Figure 5 and Table 2 below.

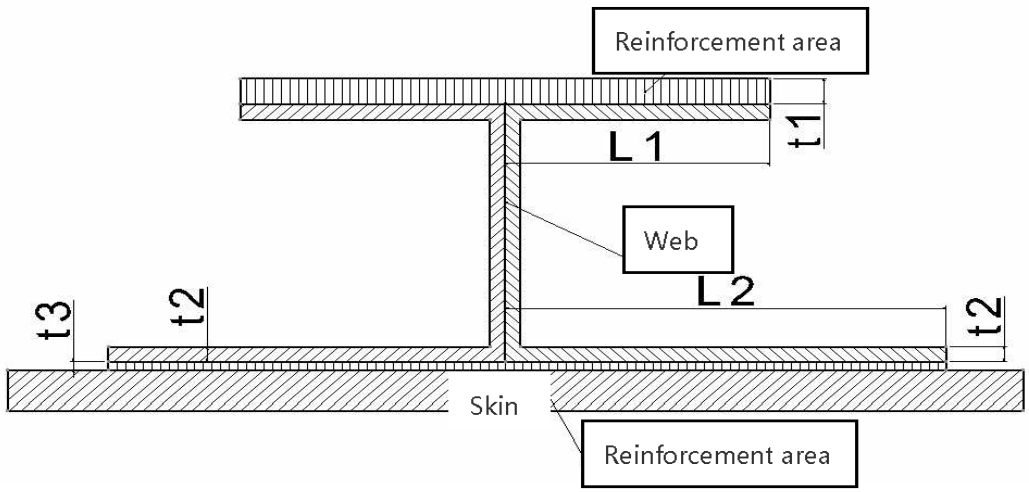

Figure 5. The cross-section of the I-shaped beam.

Table 2. Lamination information of the I-shaped beam.

Items	Parameters
Lamination, ° (t1)	[+45/−45/0/0/0/−45/0/0/0/+45]
Thickness, mm (t1)	1.85
Web lamination, ° (2 × t2)	[+45/−45/0/0/−45/0/0/+45]
Thickness, mm (2 × t2)	2.96
Flange lamination, ° (t2)	[+45/−45/0/0/−45/0/0/+45]
Flange thickness, mm (t2)	1.48
Reinforcement area, °	[±45]
Flange thickness, mm (t3)	0.37
L1, mm	13
L2, mm	23
L3, mm	23
H, mm	30
H(total), mm	35.18

2.2. Analysis Principle

In this paper, the vibration of the I-shaped beam is analyzed under various dynamic conditions (Case 1 and Case 2).

2.2.1. Modal Analysis

Modal analysis is one of the most thoughtful methods that enables the study of the dynamic performance of structures. The modal characteristics include the natural frequency and modal shape. Modal analysis is not merely the basis of the structural dynamic design, vibration control, and fault diagnosis but also is an effective way to study various structural vibrations. The equation of motion for a multi-degree-of-freedom system without constraints is illustrated below [14]:

$$[M]\{\ddot{u}\} + [K]\{u\} = 0 \tag{1}$$

where M represents the mass matrix, and K is the stiffness matrix.

2.2.2. Frequency Response Analysis

Frequency response analysis is a method that looks at the dynamic response of structures under steady-state excitation. It is usually employed to understand the dynamic response of a forced vibration excitation system. By frequency response analysis, the excitation varies with the frequency. There are two classical types of frequency response analysis methods: direct methods and modal methods. The direct method requires the integration of the frequency response function directly in the physical space, while the modal method requires obtaining the frequency response function by the linear superposition of the modes in the modal space. Compared with the direct method, the modal frequency response calculation requires less memory, exhibits higher efficiency, and makes the obtained response curve over frequency smoother and more accurate.

In the frequency domain of the finite element discrete system, the general form of the dynamic equation is shown in Equation (2) [14]:

$$\left(-\omega^2 \mathrm{M} + \mathrm{i}\omega \mathrm{B} + \mathrm{K}\right)\mathrm{U}(\omega) = \mathrm{F}(\omega) \tag{2}$$

In the formula, M is the mass matrix, B is the damping matrix, and K is the stiffness matrix of the n-degree-of-freedom system. In direct frequency response analysis, Equation (3) [14] is solved for a coupled multi-degree-of-freedom system. However, in modal frequency response analysis, it is transformed to modal coordinates and solved by uncoupled one-degree-of-freedom equations.

$$\left(-\omega^2 m_i + \mathrm{i}\omega b_i + k_i\right)u_i(\omega) = f_i(\omega) \tag{3}$$

In the formula, m_i are the modal masses, b_i are the modal damping values, and k_i are the transformed single-degree-of-freedom modal stiffnesses.

2.2.3. Random Response Analysis

Aircraft structures under non-stationary random excitation generate a dynamic response affected by a large number of factors. The random vibration component tends to increase or decrease under different flight statuses and frequency ranges. Random vibration is a kind of uncertain and irregular vibration, which cannot be expressed or described by deterministic time and space functions but only by statistical probability distributions. Founded on the theory of random process and the method of frequency domain analysis, the dynamic response of structures under random vibration excitation is described by the power spectral density (PSD) function.

The PSD function of the acceleration response in the region where the damage failure occurs can be given in Equation (4) [14]:

$$\mathrm{G(f)} = \mathrm{W(f)}H^2(f) \tag{4}$$

In the formula, H(f) is the frequency response vector, and W(f) is the power spectral density function (PSD) with the input random acceleration. The n-order spectral moment of inertia of the PSD function is described in Equation (5) [14]:

$$J_n = \int_0^\infty f^n G(f) df \tag{5}$$

When n = 0, J_0 can be given as the area of the lower region surrounded by the PSD curve. Thus, the RMS (root mean square) value of the stochastic process can be achieved as in Equation (6) [14]:

$$\mathrm{RMS} = \sqrt{J_0} \tag{6}$$

2.3. Dynamic Analysis Results

The results of the dynamic analysis provide information on the performance of the system subjected to vibration excitation.

As the scope of the paper is to identify the best possible location of the clamping elements used during cutting, we need to look at the frequency response of the system when the clamping points are at different locations. Dissimilar results of strain and stress will reveal the existence of the best possible positions of the clamping points for the machining part. Hence, the following analysis will investigate the 1st to 10th mode shapes of the beam. The cutting tool's rotation speed is 5000 r/min. The natural frequency is around 83.3344 Hz.

2.3.1. Modal Analysis Results

In the modal analysis of MSC.NASTRAN SOL103, Case 1's frequency and vibration modes are shown in Figures 6–15 for a beam with an I cross-section.

In the modal analysis of MSC.NASTRAN SOL103, Case 2's frequency and vibration modes are shown in Figures 16–25.

From Figures 6–25, Case 1 and Case 2 present the same intrinsic modal vibration pattern. The frequencies under 1000 Hz in Case 2 are significantly higher than those of Case 1. However, Case 1 has some frequencies higher than those of Case 2 when the frequency is higher than 1000 Hz. The lowest frequency of Case 1 is 546.63 Hz, while that of Case 2 is 848.19 Hz, which are considerably higher (about 7- and 10-times higher) than the natural frequency of 83.33 Hz of the cutting tool. See Table 3 for comparison values of frequencies.

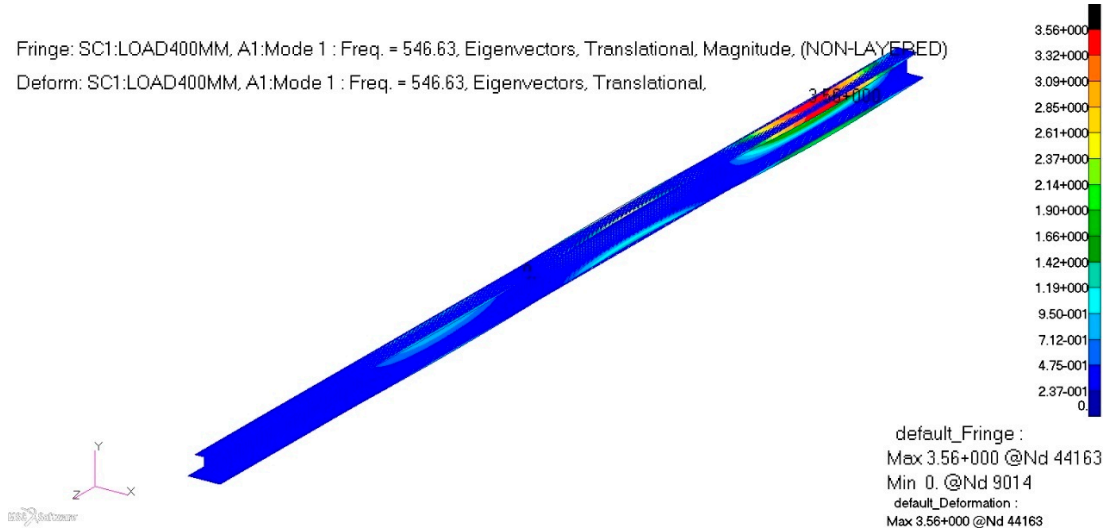

Figure 6. 1st mode.

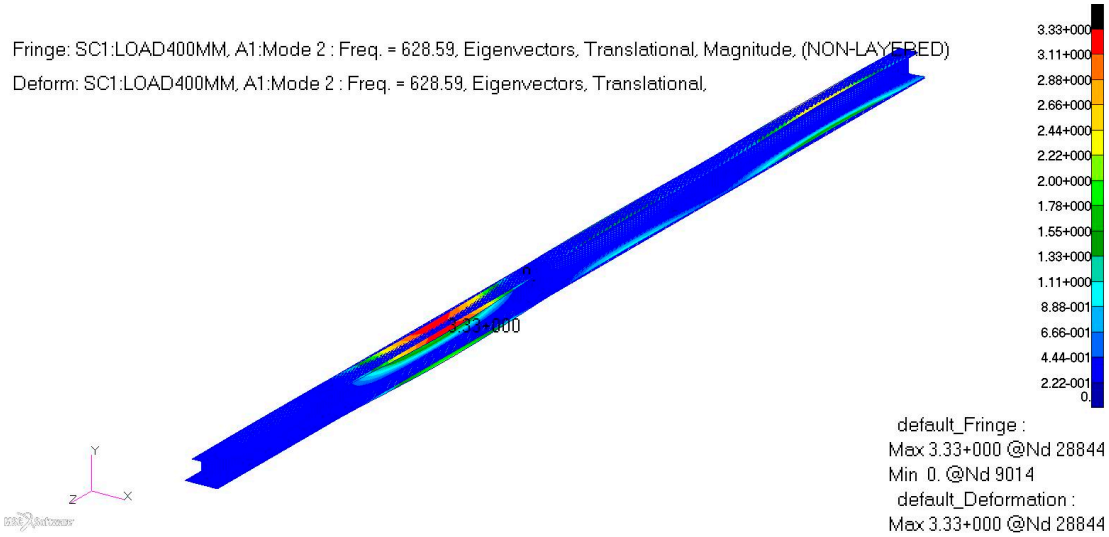

Figure 7. 2nd mode.

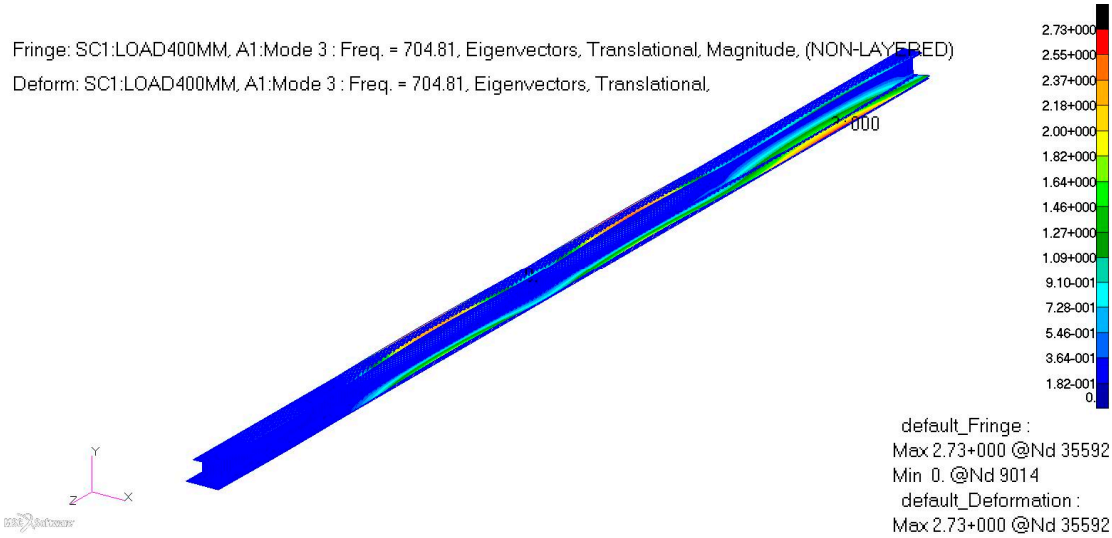

Figure 8. 3rd mode.

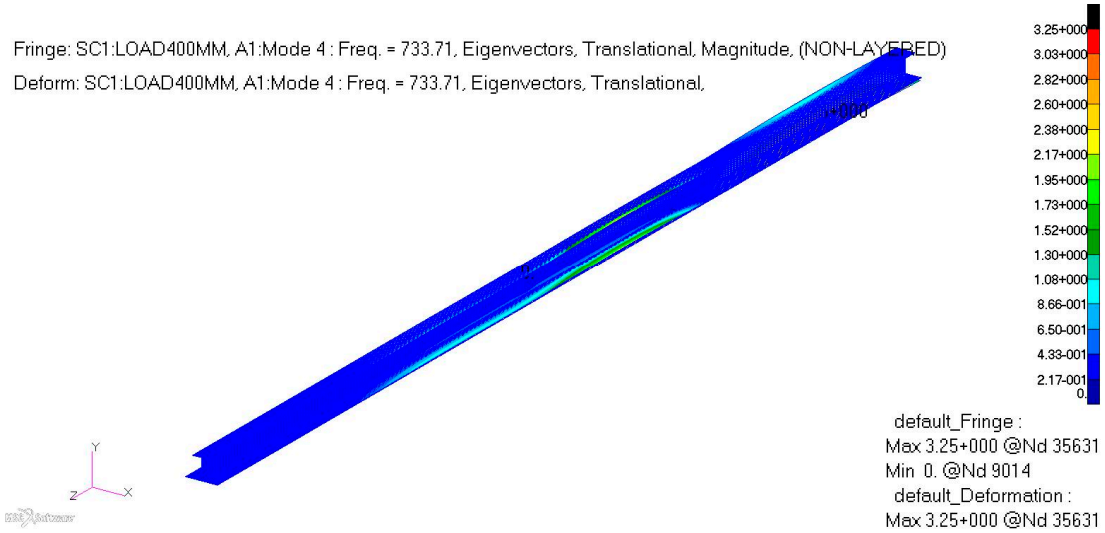

Figure 9. 4th mode.

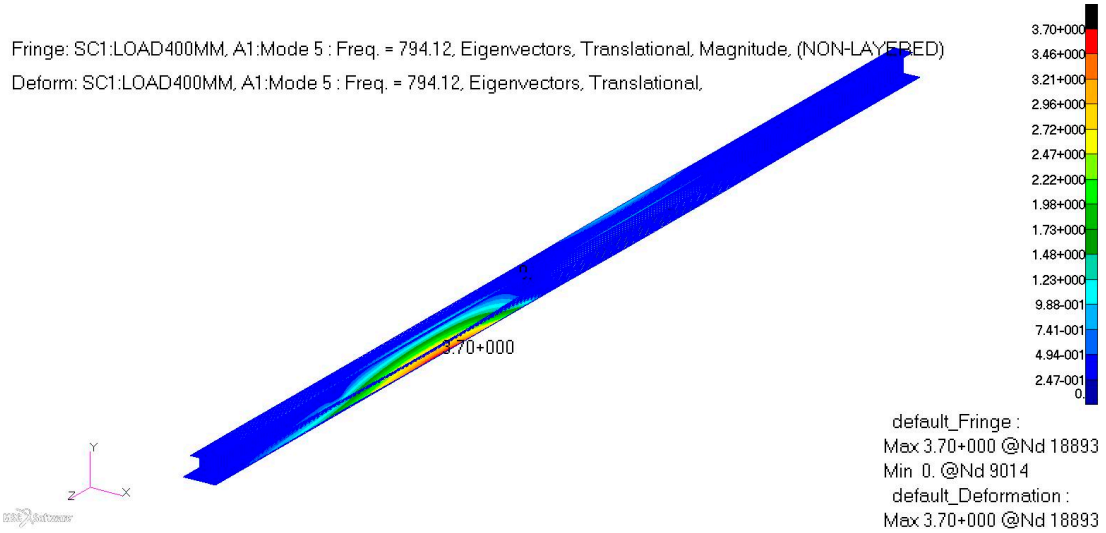

Figure 10. 5th mode.

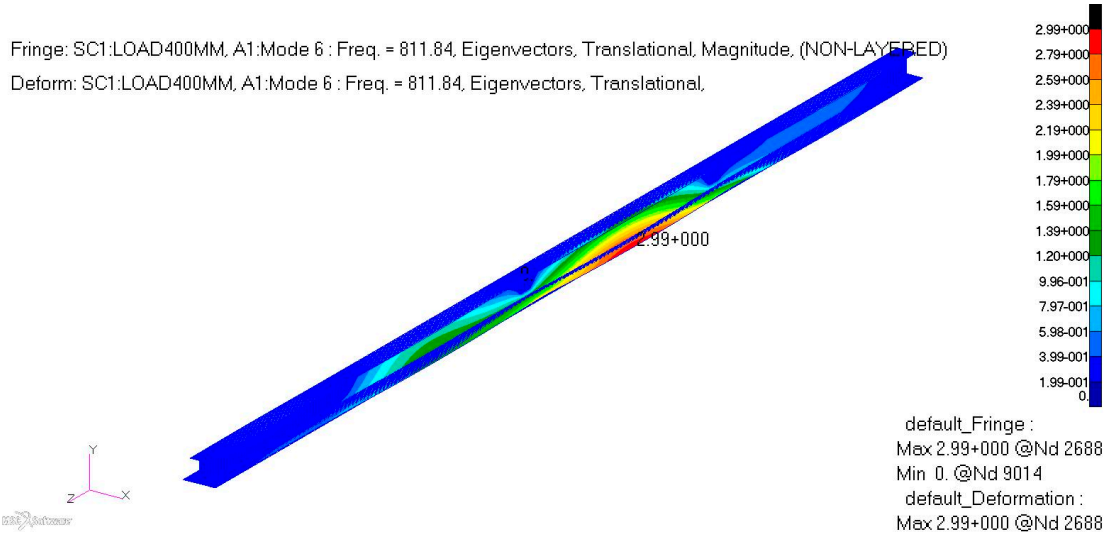

Figure 11. 6th mode.

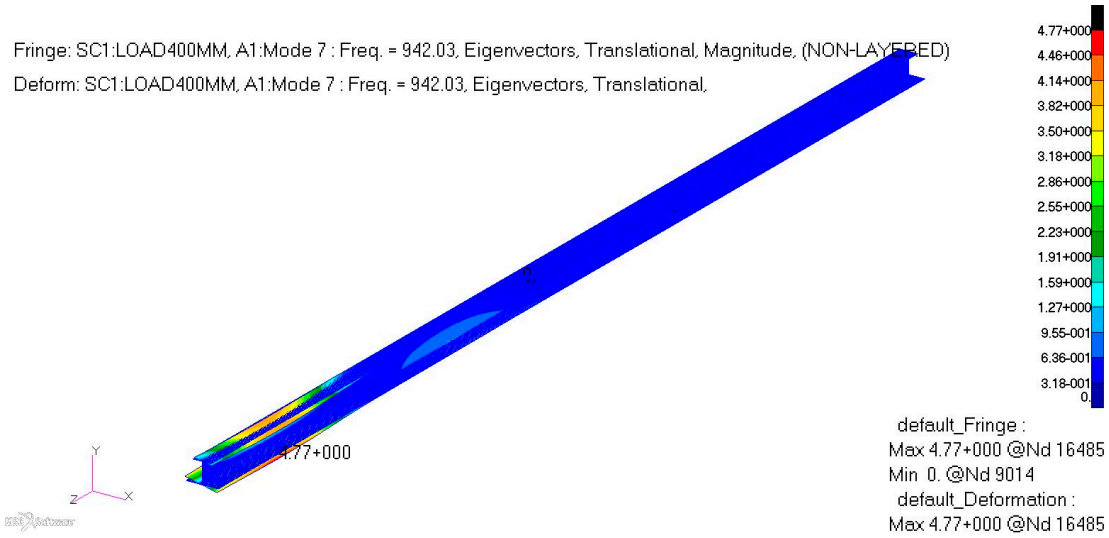

Figure 12. 7th mode.

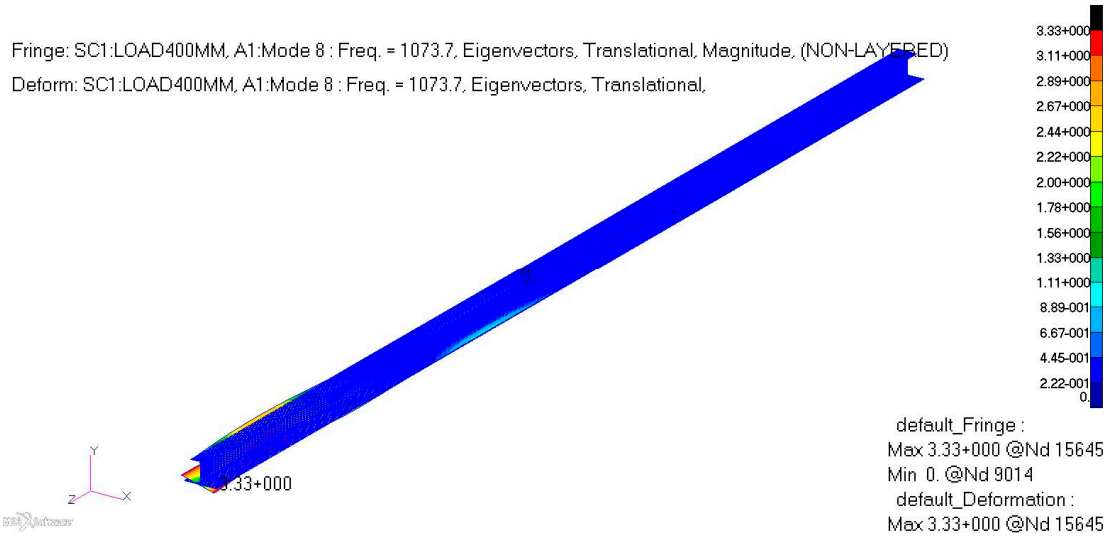

Figure 13. 8th mode.

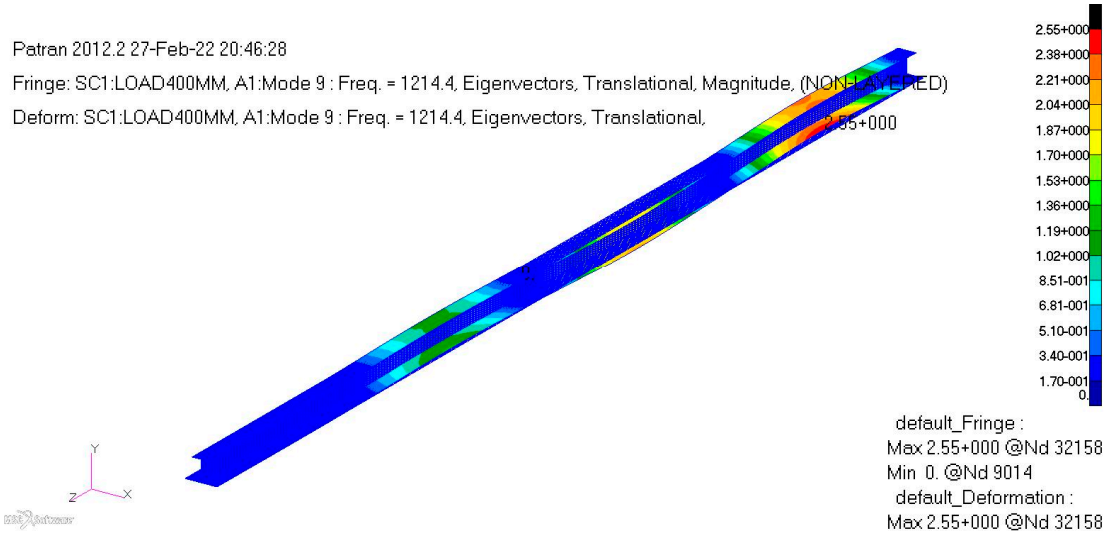

Figure 14. 9th mode.

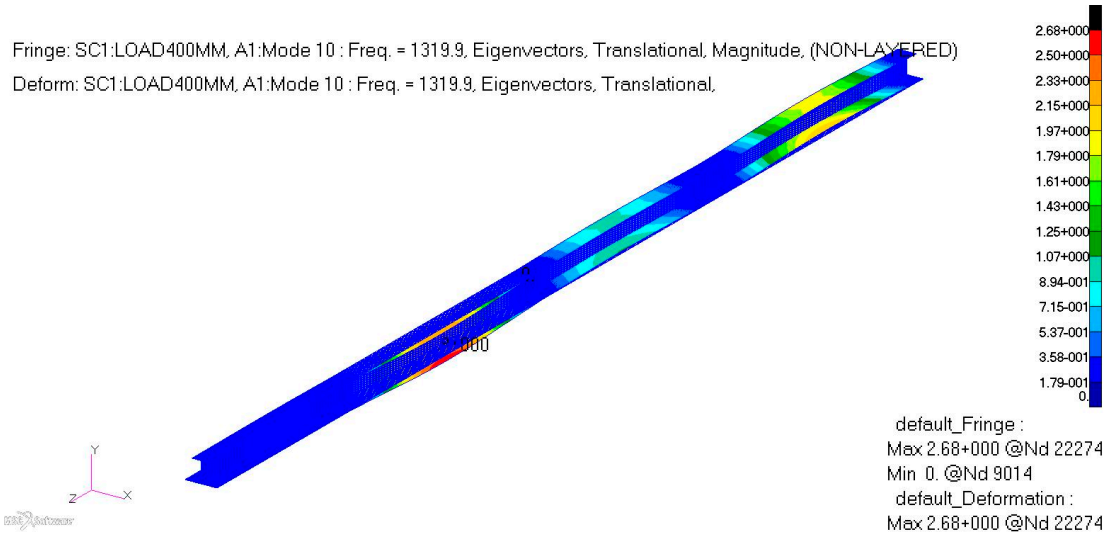

Figure 15. 10th mode.

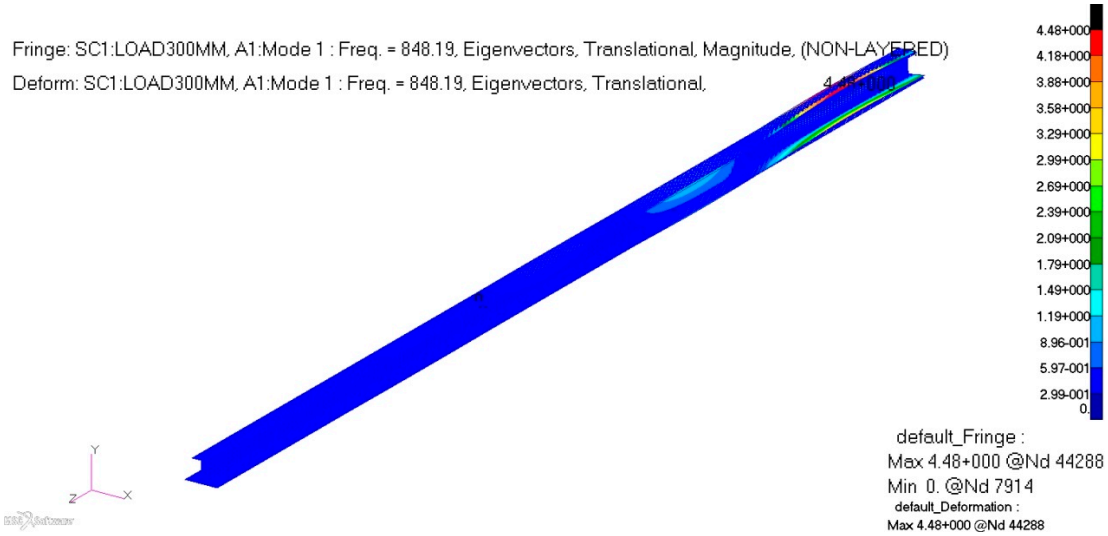

Figure 16. 1st mode.

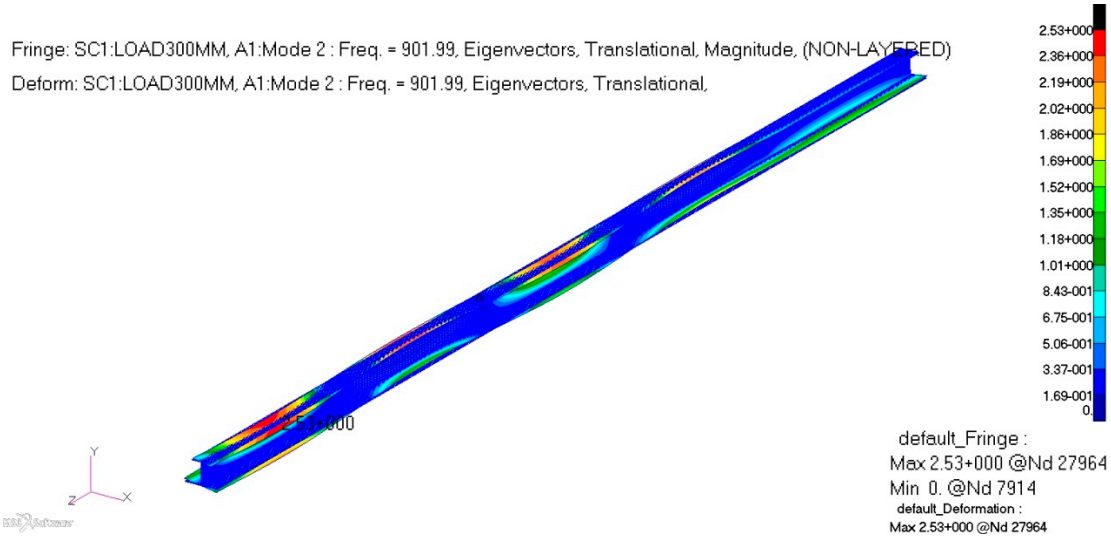

Figure 17. 2nd mode.

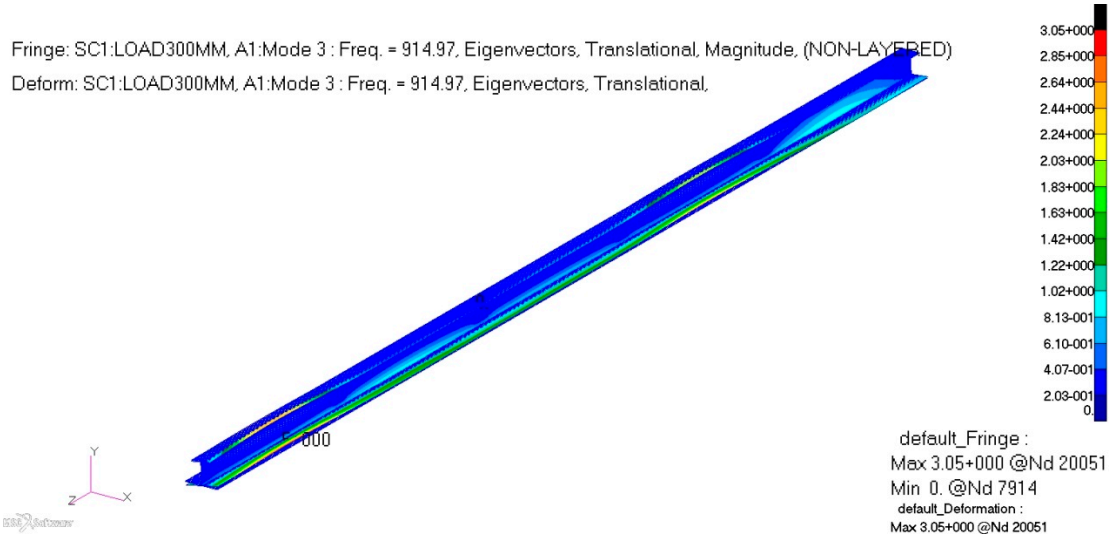

Figure 18. 3rd mode.

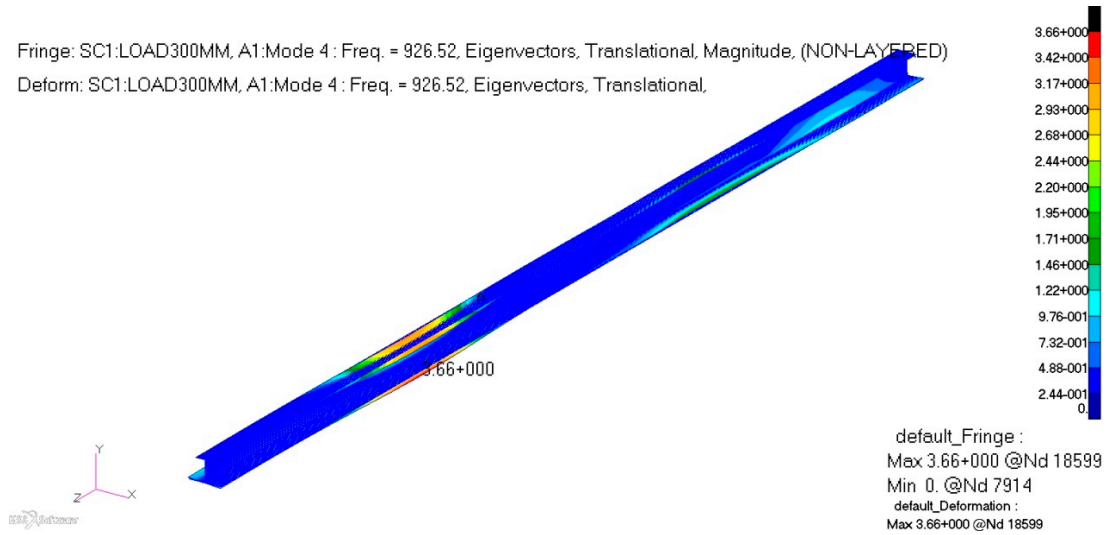

Figure 19. 4th mode.

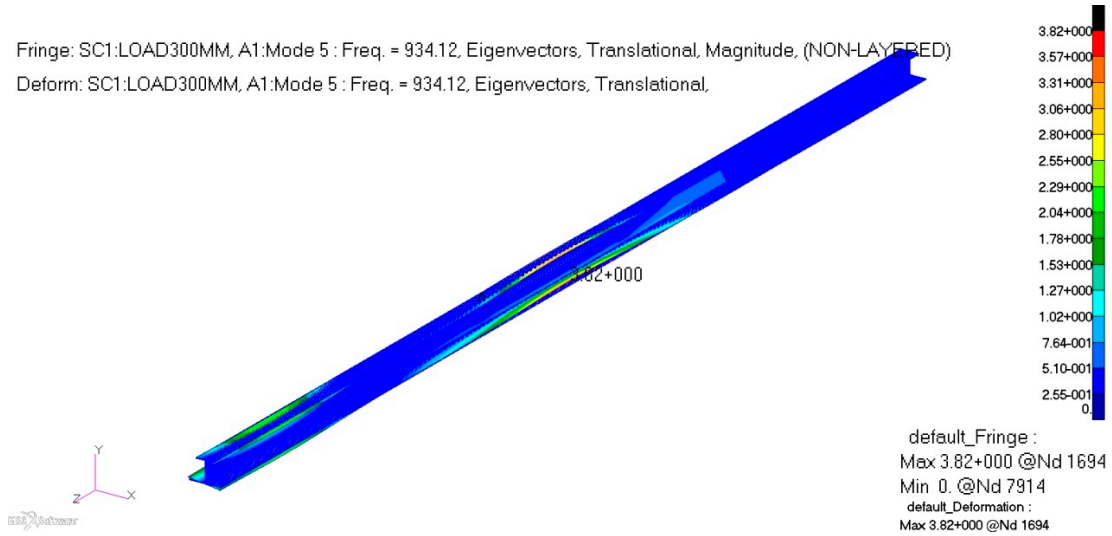

Figure 20. 5th mode.

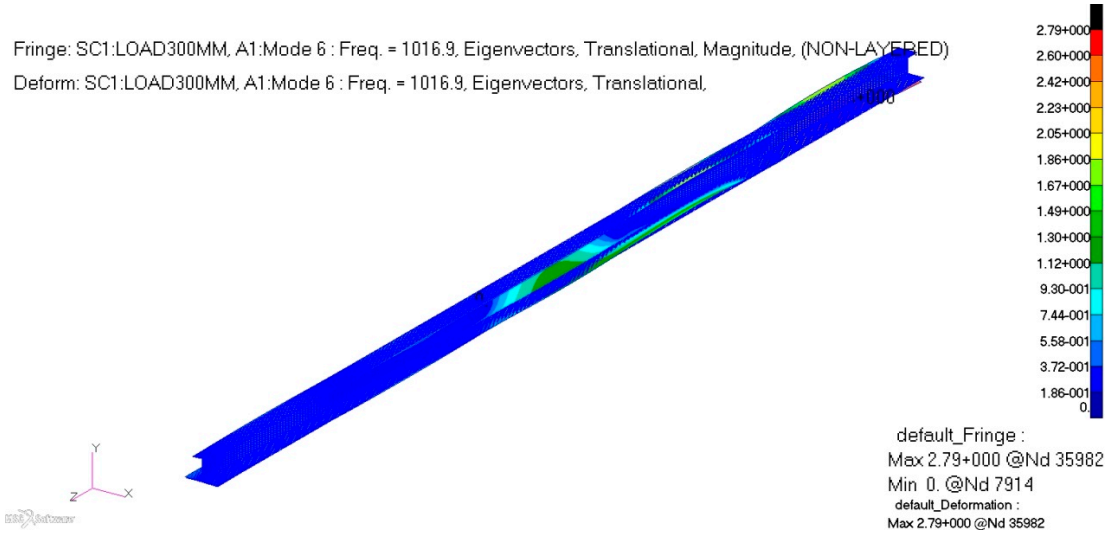

Figure 21. 6th mode.

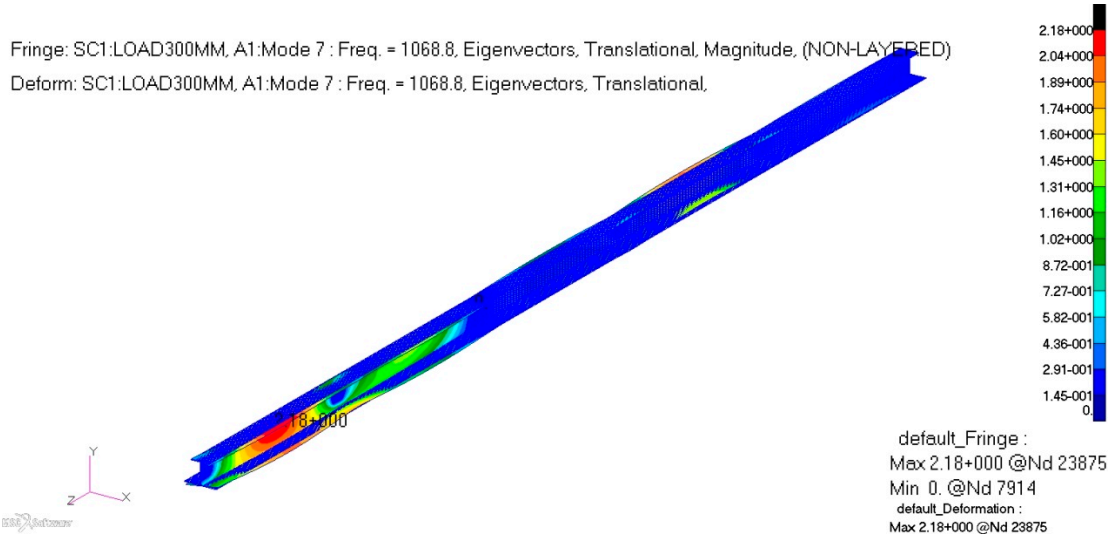

Figure 22. 7th mode.

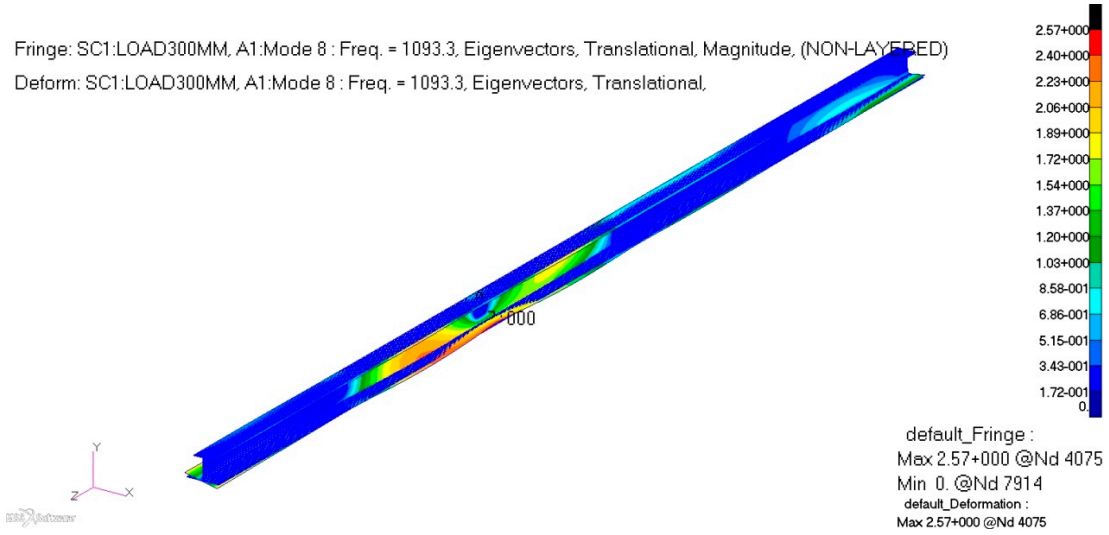

Figure 23. 8th mode.

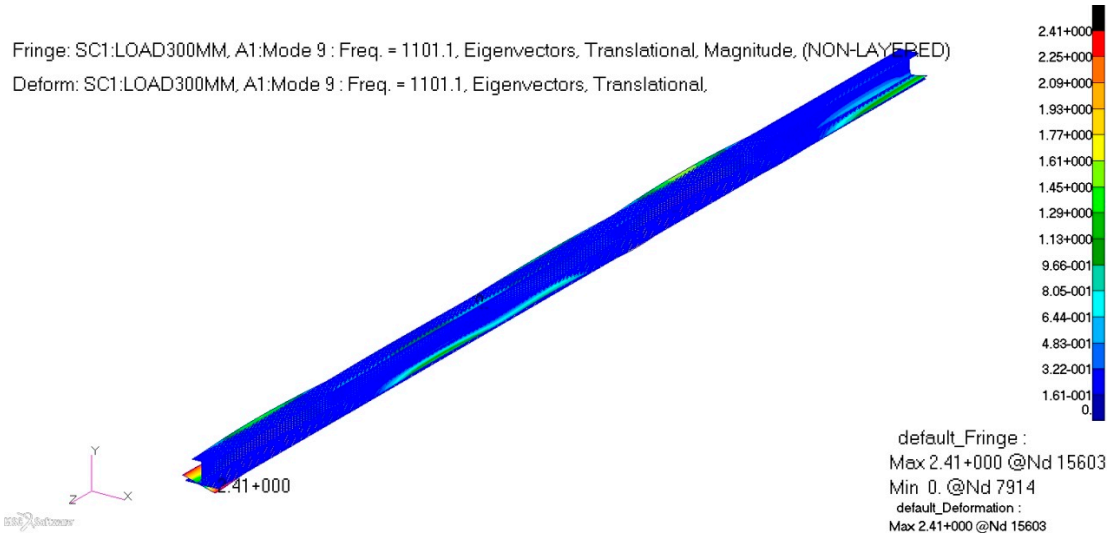

Figure 24. 9th mode.

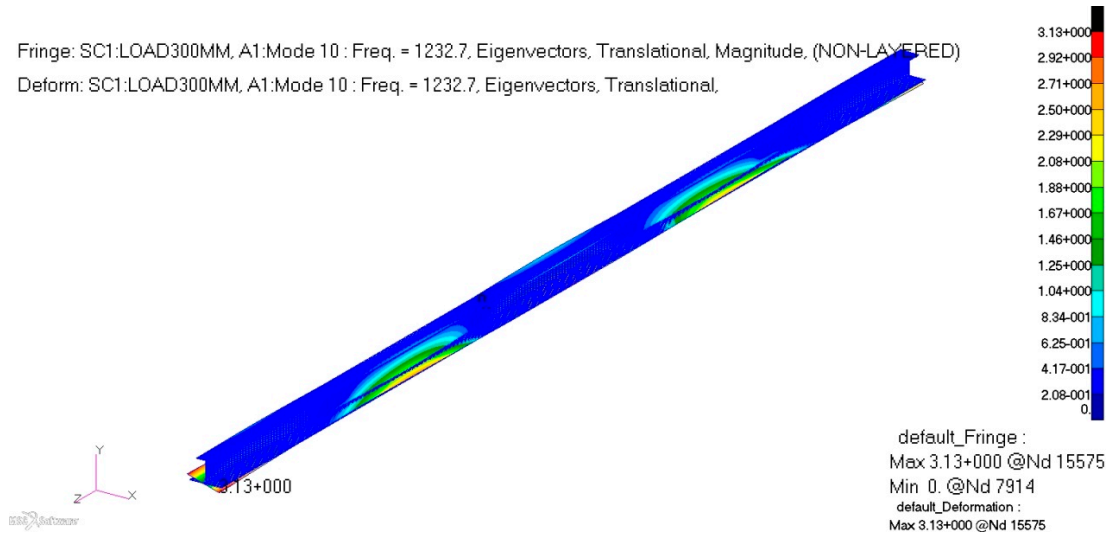

Figure 25. 10th mode.

Table 3. Comparison frequencies of Case 1 vs. Case 2.

Cases	Case 1 (Hz)	Case 2 (Hz)	Differences (%)
1st mode	546.63	848.19	↑ 55.16711
2nd mode	628.59	901.99	↑ 43.49417
3rd mode	704.81	914.97	↑ 29.81797
4th mode	733.71	926.52	↑ 26.27877
5th mode	794.12	934.12	↑ 17.62958
6th mode	811.84	1016.9	↑ 25.25867
7th mode	942.03	1068.8	↑ 13.45711
8th mode	1073.7	1093.3	↑ 1.825463
9th mode	1214.4	1101.1	↓ 9.32971
10th mode	1319.9	1232.7	↓ 6.60656

2.3.2. Results of Frequency Response Analysis

An equal 1-unit impact sine load is applied to the upper flange of the I-shaped beam with different spacing of the fixture. MSC.NASTRAN SOL111 is utilized to solve these dynamic models (See Figures 3 and 4). The results are shown in Figures 26–37.

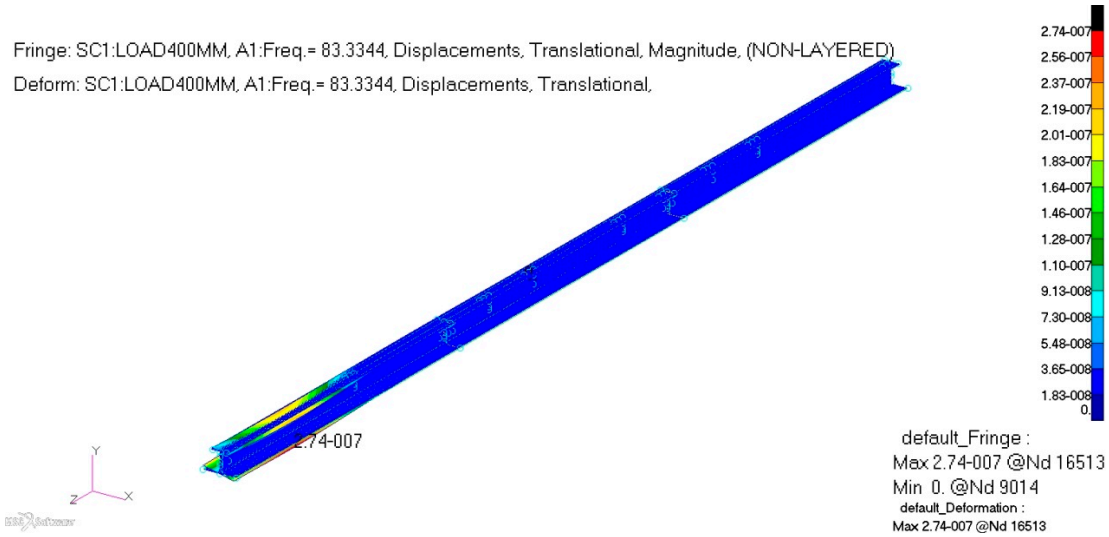

Figure 26. Vibration displacement of the I-shaped beam in Case 1 (f = 83.3344 Hz).

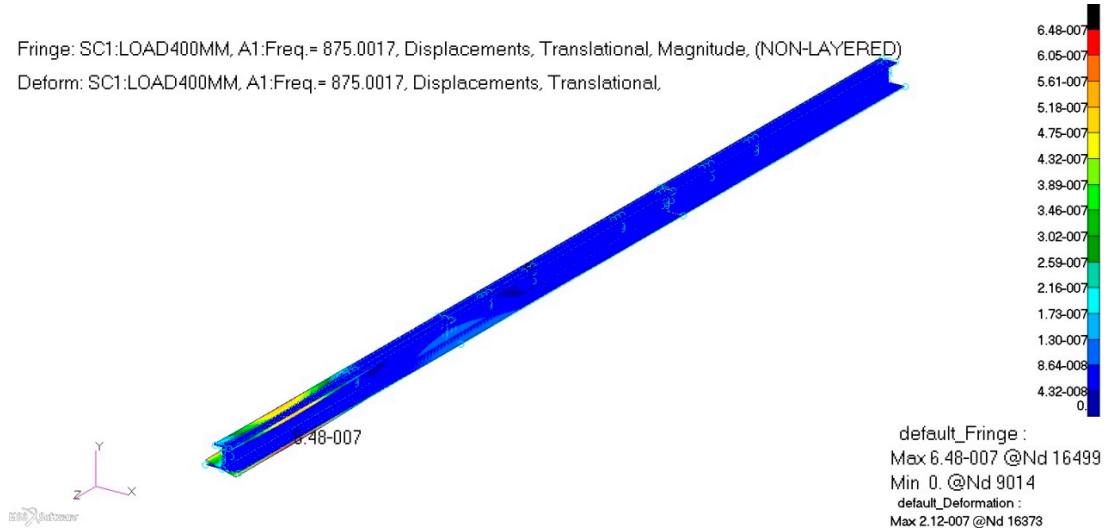

Figure 27. Vibration displacement of the I-shaped beam in Case 1 (f = 875.00174 Hz).

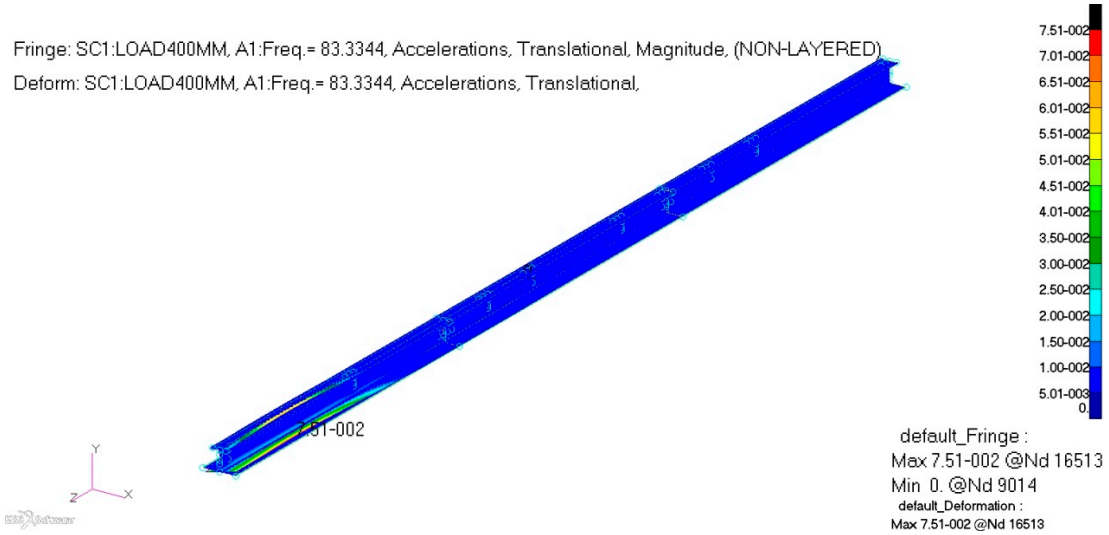

Figure 28. Vibration acceleration of the I-shaped beam in Case 1 (f = 83.3344 Hz).

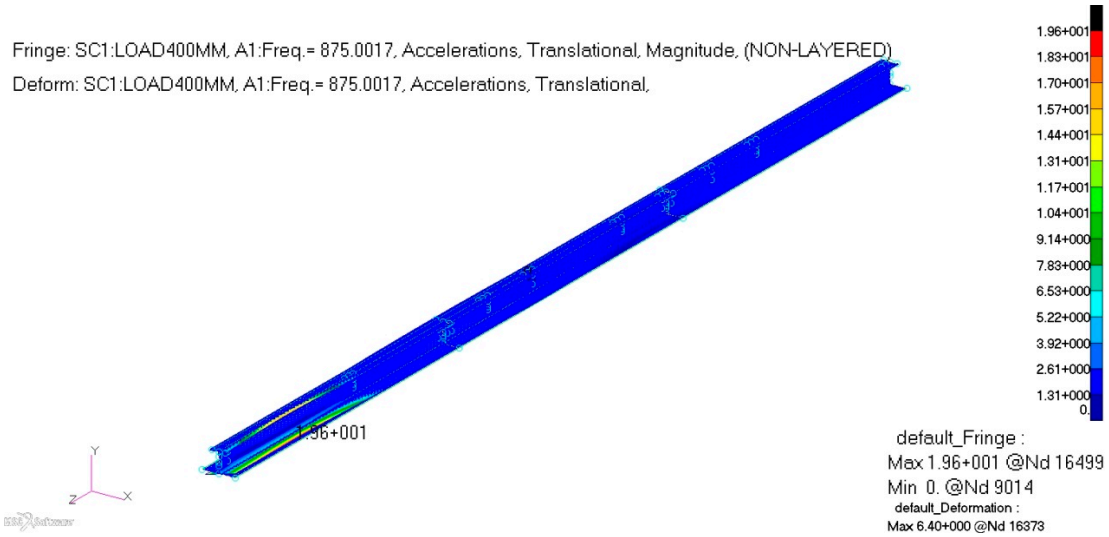

Figure 29. Vibration acceleration of the I-shaped beam in Case 1 (f = 875.0017 Hz).

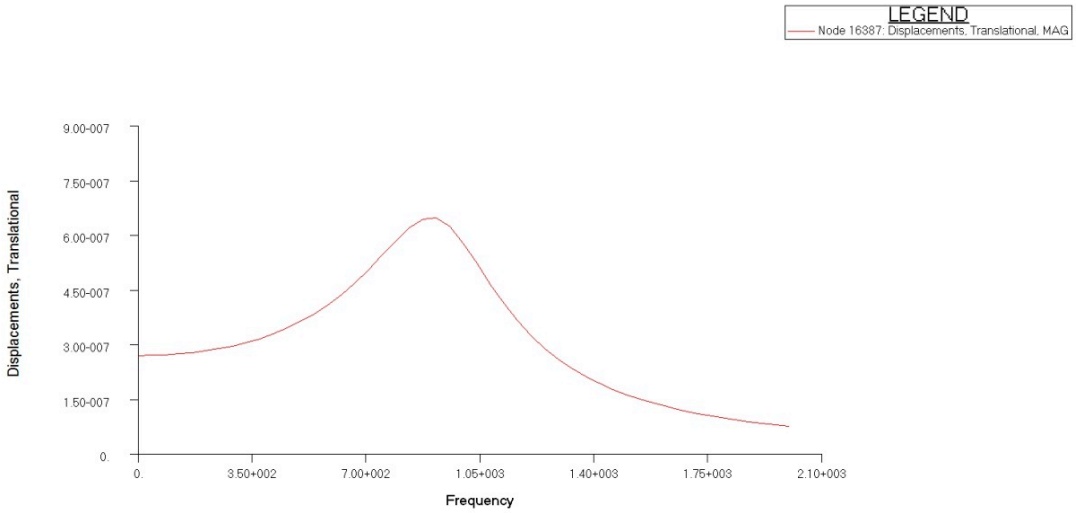

Figure 30. Typical node displacement with frequency for Case 1.

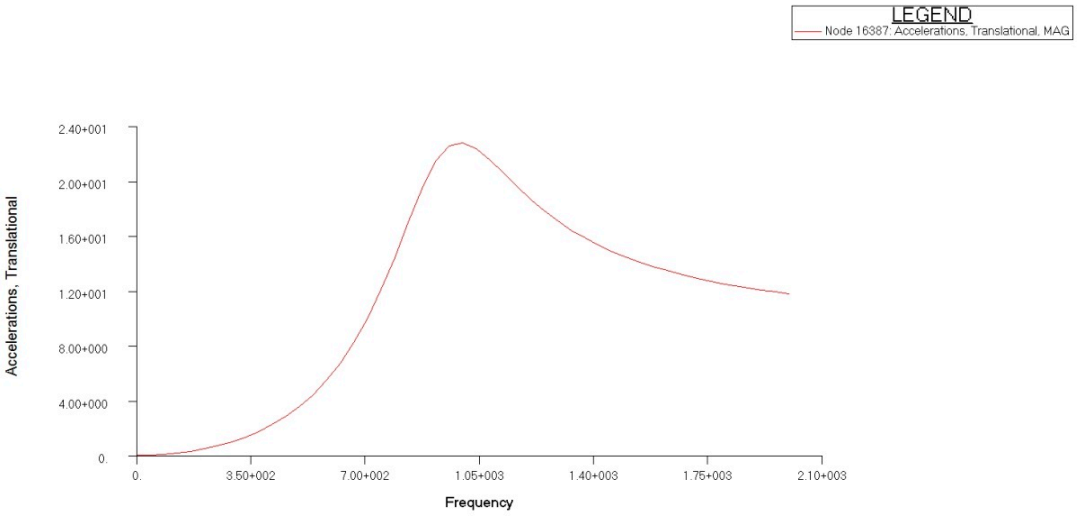

Figure 31. Typical node acceleration with frequency for Case 1.

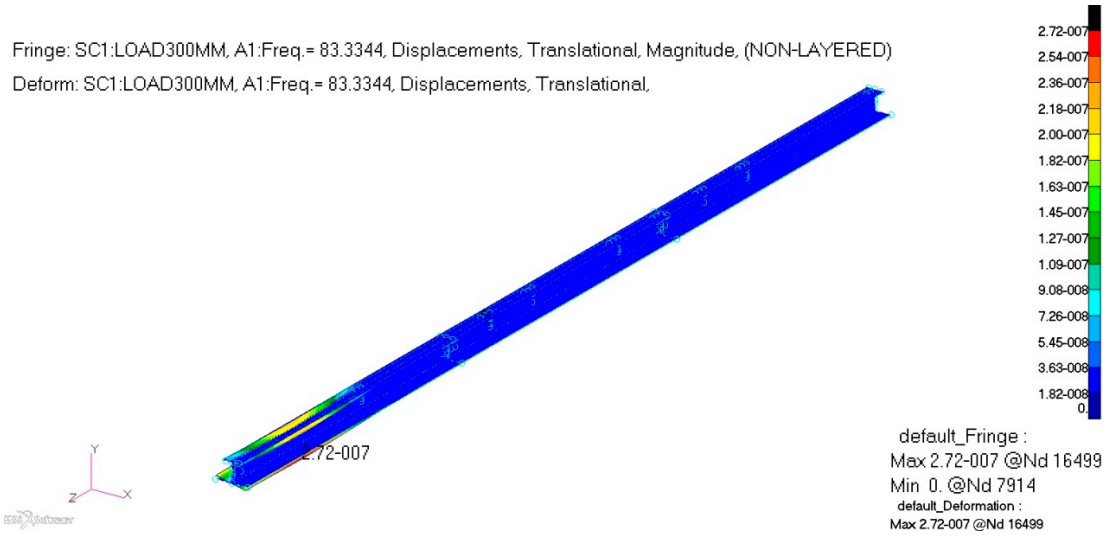

Figure 32. Vibration displacement of the I-shaped beam in Case 2 (f = 83.3344 Hz).

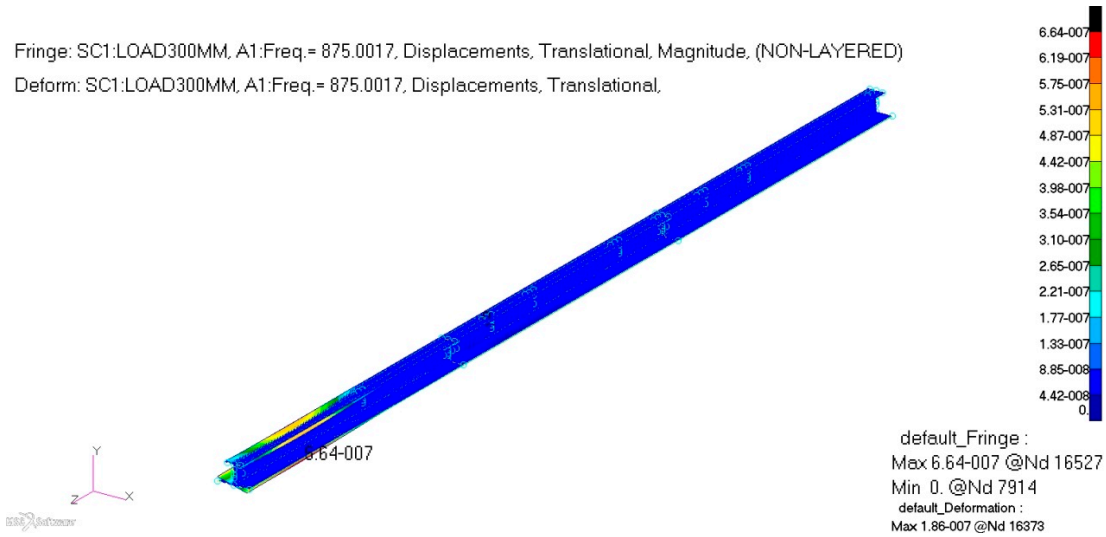

Figure 33. Vibration displacement of the I-shaped beam in Case 2 (f = 875.0017 Hz).

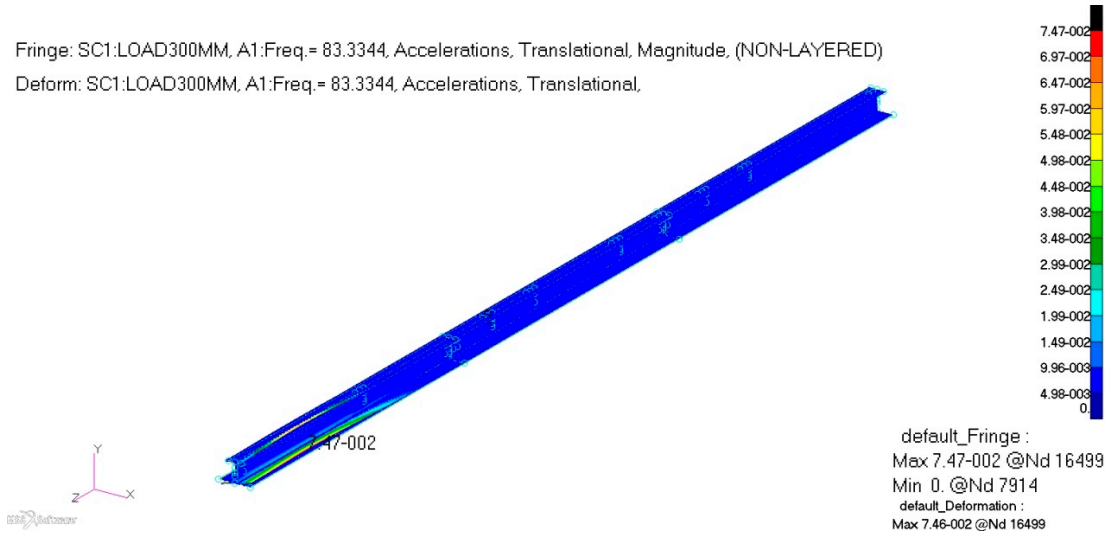

Figure 34. Vibration acceleration of the I-shaped beam in Case 2 (f = 83.3344 Hz).

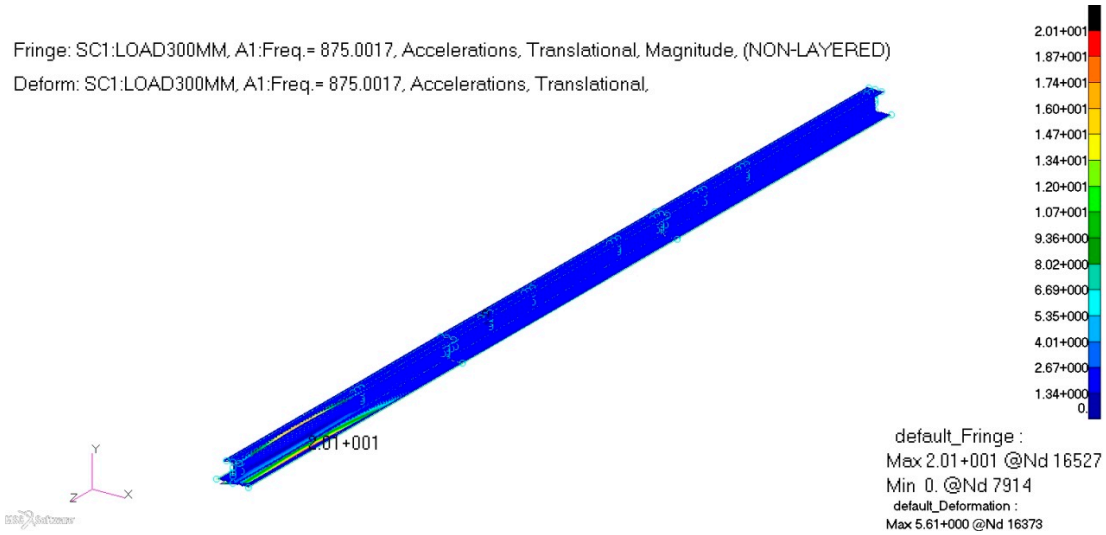

Figure 35. Vibration acceleration of the I-shaped beam in Case 2 (f = 875.0017 Hz).

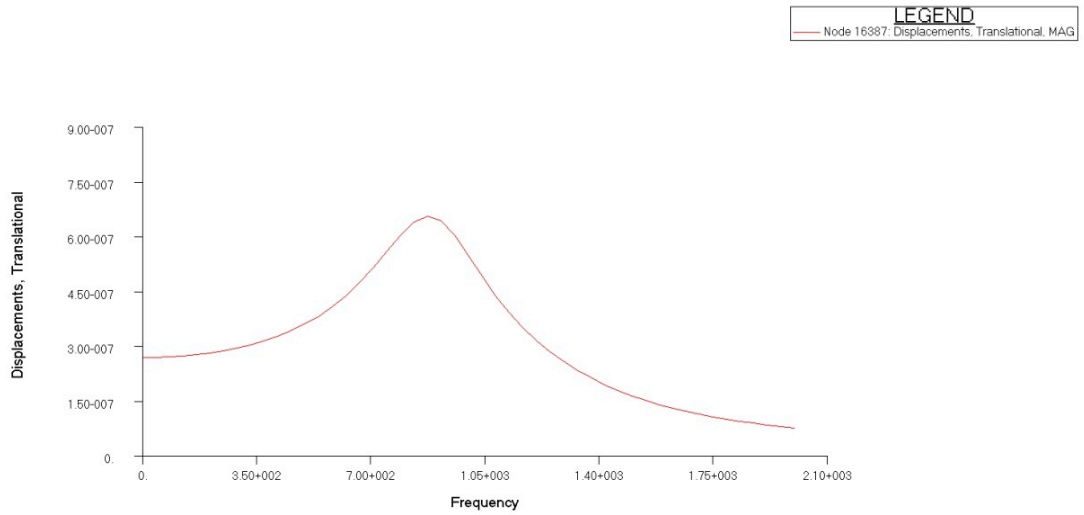

Figure 36. Typical node displacement with frequency for Case 2.

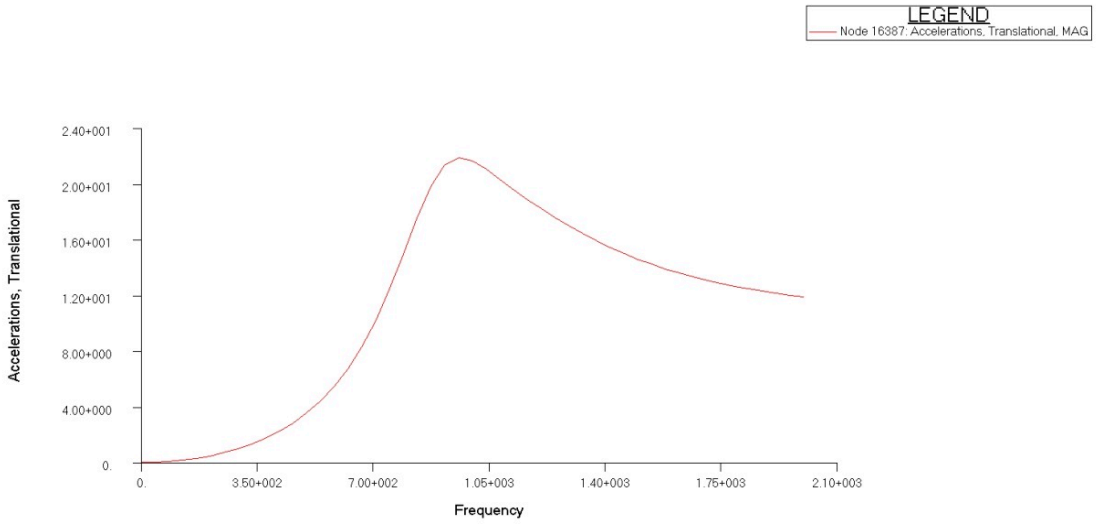

Figure 37. Typical node acceleration with frequency for Case 2.

The displacement and acceleration at the same frequency with different spacing fixtures are shown in Table 4. Based on Case 1, the result data are normalized.

Table 4. Comparison of the displacement and acceleration of the workpiece.

Cases	Displacement (m)	Acceleration (m/s^2)	Frequency (Hz)
Case 1	1.0	1.0	83.3344
Case 2	0.9927	0.9947	
Case 1	1.0	1.0	875.0017
Case 2	1.0247	1.0255	

According to the dynamic responses of Case 1 and Case 2, the vibration displacement and acceleration of Case 1 are slightly higher than those of Case 2 at the frequency of 83.33 Hz. The peak frequency of the vibration displacement and acceleration of Case 1 and Case 2 is about 870 Hz, while the max values of the vibration displacement and acceleration of Case 2 are slightly larger than those of Case 1. The results show that a reduction in the fixed distance (Case 2) cannot reduce the vibration of the workpiece.

2.3.3. Random Response Analysis Results

After the frequency response analysis of Case 1 and Case 2, white noise is implemented to analyze the random response. Figures 38–41 show the consequences of this analysis.

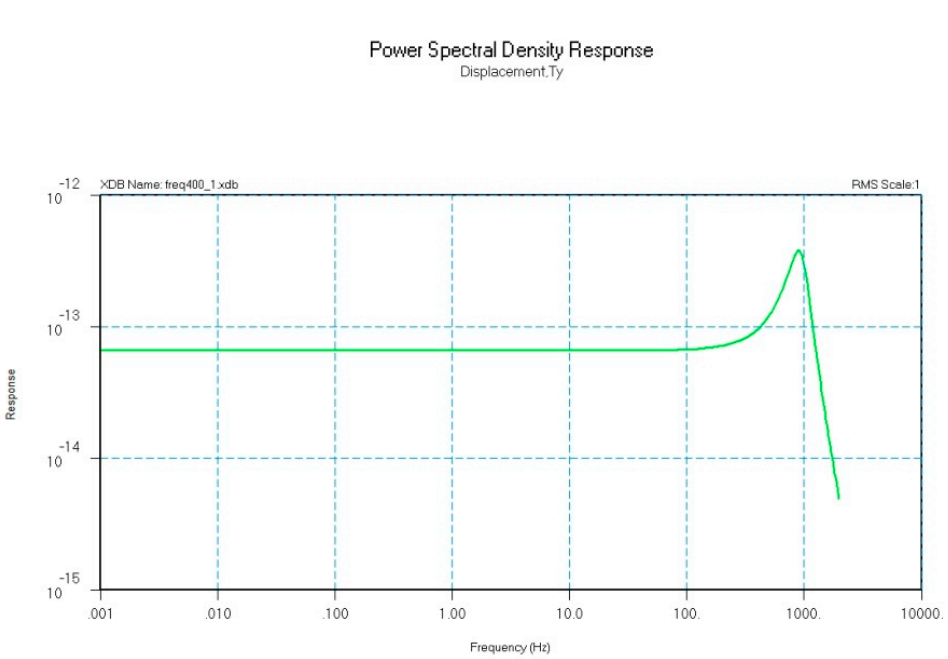

Figure 38. PSD response along *y*-axis displacement of the typical node in Case 1.

From the 2000 Hz frequency's sweep, one could find that the PSD peak of the vibration displacement and acceleration (about 83 Hz) in Case 1 is almost the same as that of Case 2's vibration displacement and acceleration. At the higher frequency of 870 Hz, the max PSD of the displacement and acceleration of Case 2 is slightly higher than that of Case 1. It is explained again that shortening the clamping space of the fixture has little or no effect to restrain the vibration.

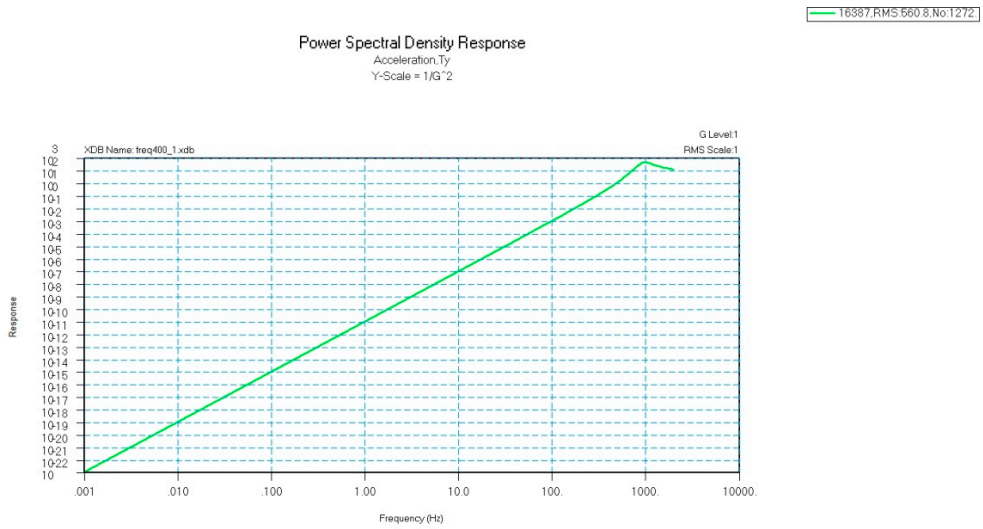

Figure 39. PSD response along *y*-axis acceleration of the typical node in Case 1.

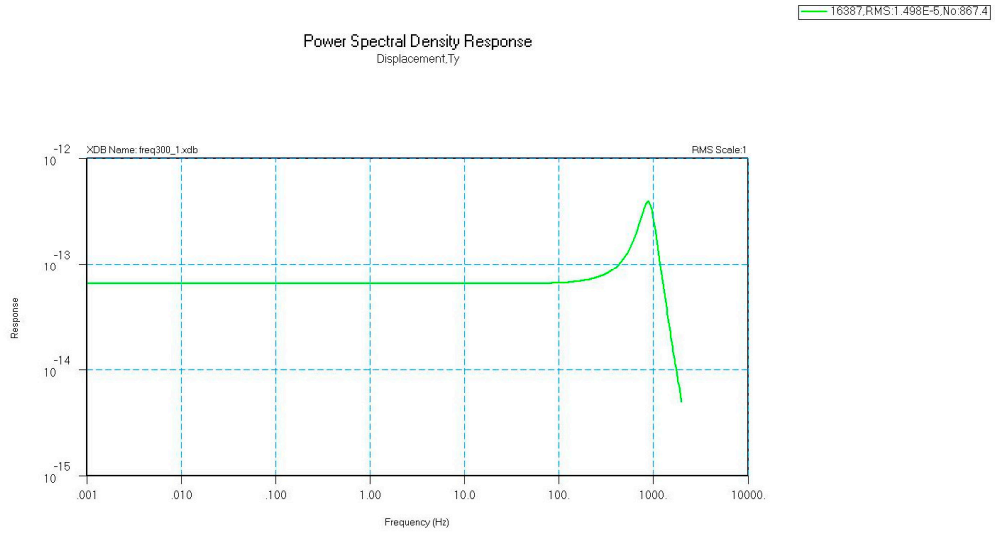

Figure 40. PSD response of *y*-axis displacement of the typical node in Case 2.

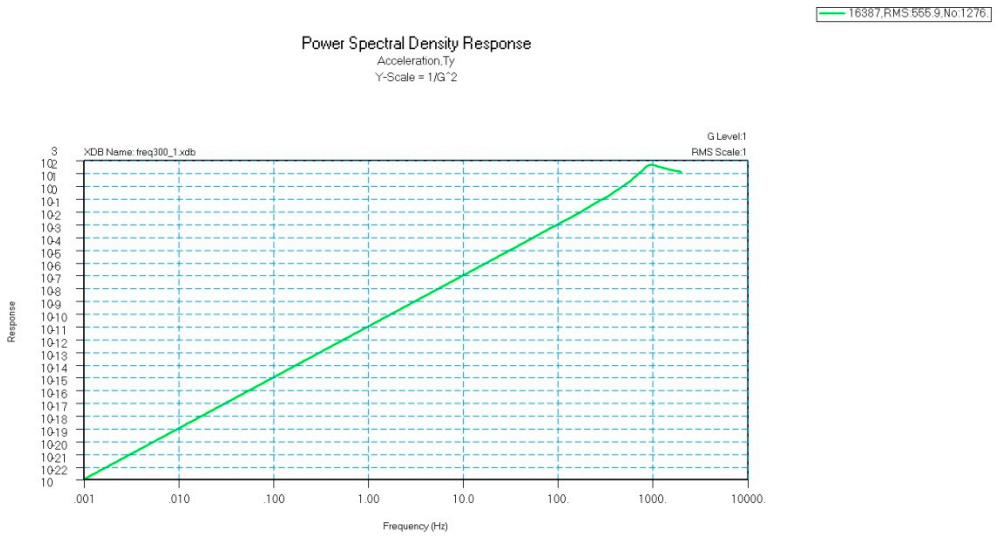

Figure 41. PSD response along the *y*-axis acceleration of the typical node in Case 1.

2.3.4. Discussion

From the above two dynamic analyses of the different clamping spacings of the fixture, although at a low frequency (<1000 Hz) the natural frequency of the workpiece can be increased in Case 2, in the high frequency range, the natural frequency of the system goes down compared with that of Case 1. From the frequency response analysis, the change in the fixture spacing in Case 2 does not reduce the vibration displacement and its acceleration, but it leads to an increase in the peak value of the PSD of the displacement and acceleration in the higher frequency.

As discussed in Section 2, it is not practicable to reduce the vibration of the workpiece during machining by shortening the holding distance at the clamping points. After some studies [15], the weak vibration position of the I-shaped beam is on the up flange of the 1/4, 1/2, and 3/4 I-shaped beam and the junction between the flange and the web. This demonstrates that weak vibration parts are related to the location and space of the fixture. At the same time, if we decrease the holding distance to 0.2 m, then two fixtures are not placed, so 0.4 m of the holding distance is chosen for the fixture.

3. The Proposed Fixture Design

Therefore, the newly designed fixture changes the holding location, which is shown in Figure 42. The profile model of the new fixture is shown in Figure 43. The design of the new fixture is based on static and dynamic analysis. Model materials and laminations are shown in Table 2 and Figure 5.

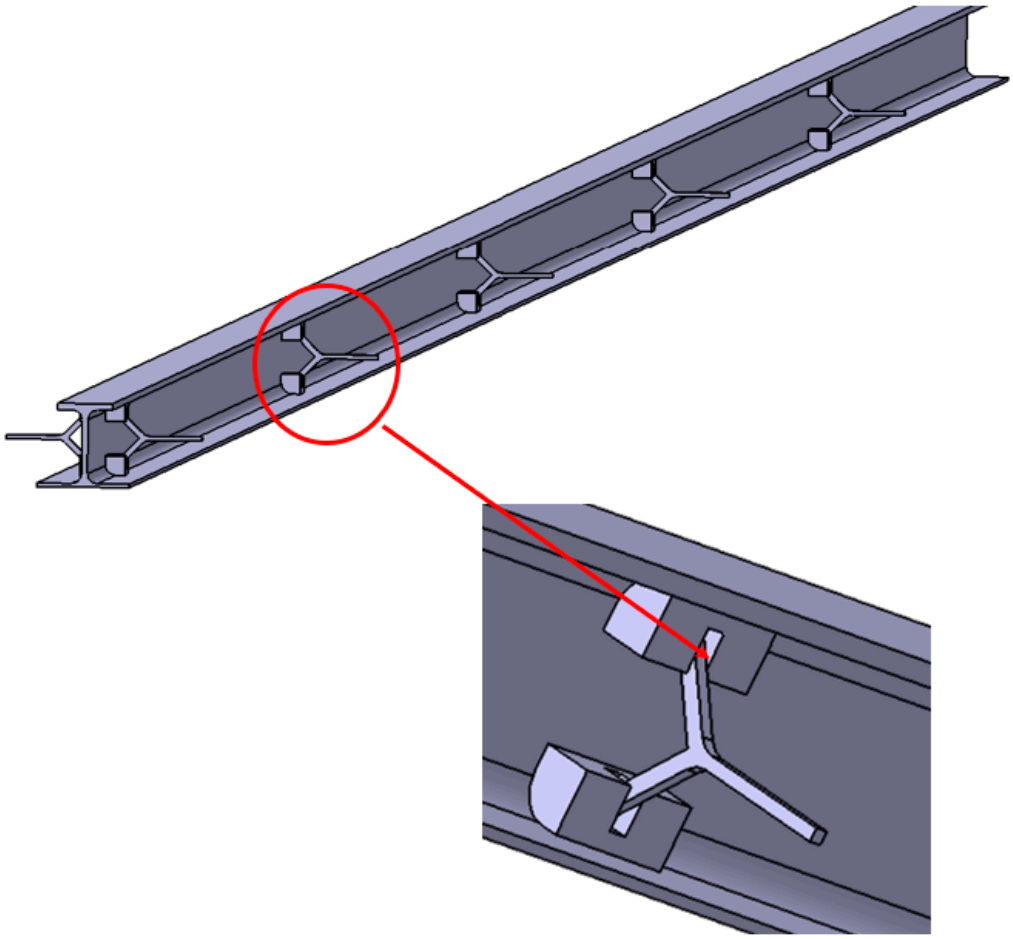

Figure 42. Schematic diagram of the new fixture.

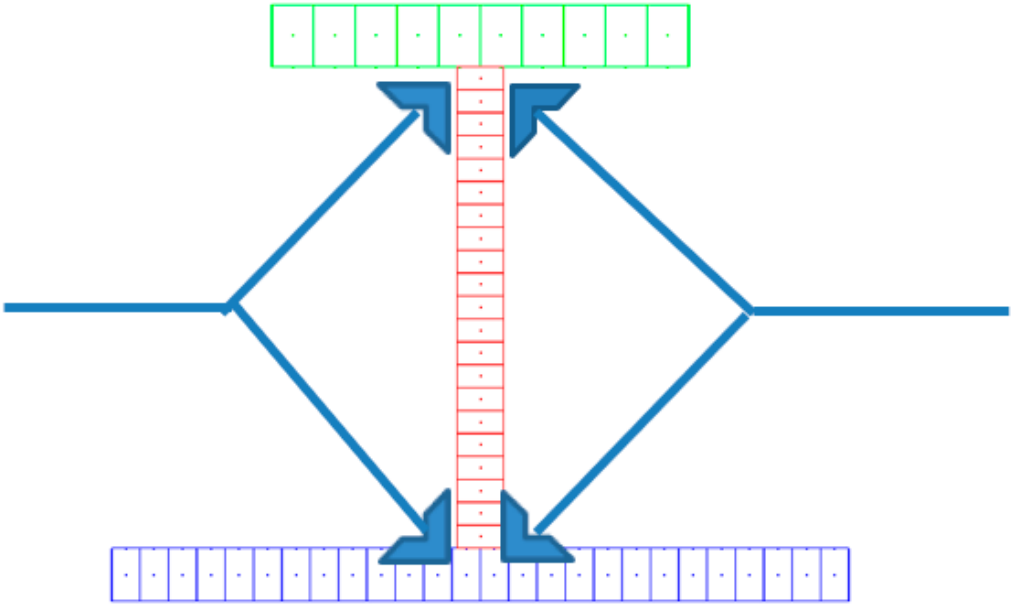

Figure 43. The proposed configuration of the clamping profile.

3.1. The Analysis Model

3.1.1. The Static Model

We have several similar beams which have different lengths, and the longest beam for the statics check here is relatively conservative. The longest workpiece is 5.8 m long, the clamping position is defined as the constraint in the model, the spacing is 0.4 m, and 100 g overload is applied at the center of gravity of the I-shaped beam according to the monitoring of the highest load during the machining process. The meshing dimension is 4 mm × 4 mm. The original fixture finite element model is presented in Figure 44 (Case 3). There are 42,395 nodes and 40,927 2-D elements. The finite element model shown in Figure 45 is developed based on the machining charts shown in Figures 42 and 43.

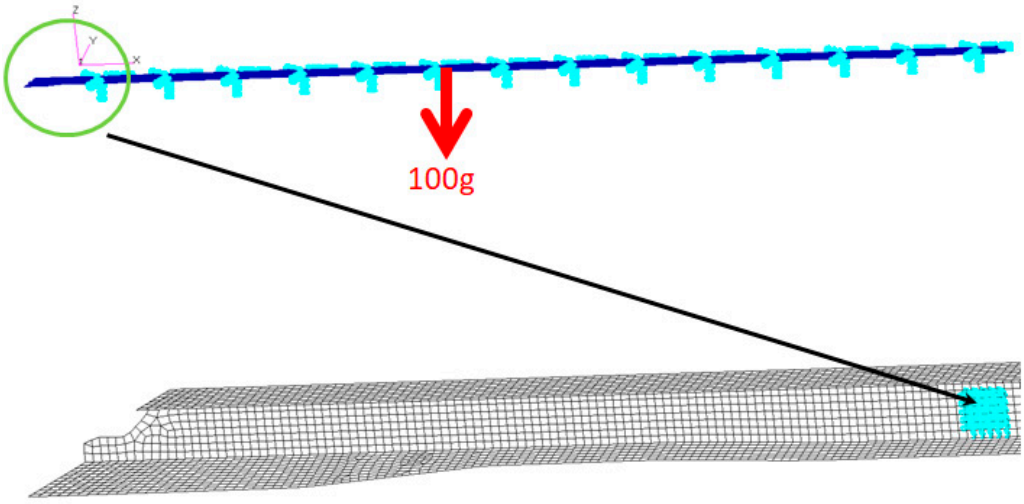

Figure 44. Original static model clamped at the web (Case 3).

3.1.2. The Dynamic Model

According to processing Figures 42 and 43, the dynamic analysis model (Case 5) of the finite element model (Figure 46) with a length of 1.5 mm is established for comparing Case 1.

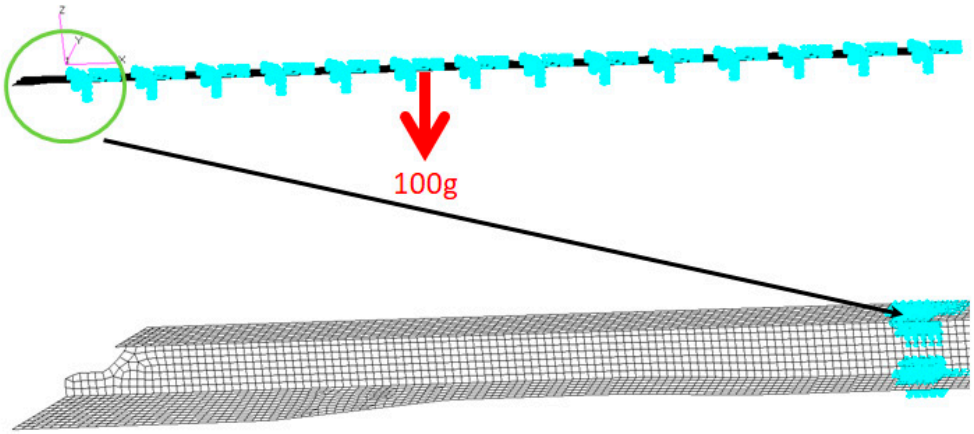

Figure 45. The static model clamped at the junction of the web and flange (Case 4).

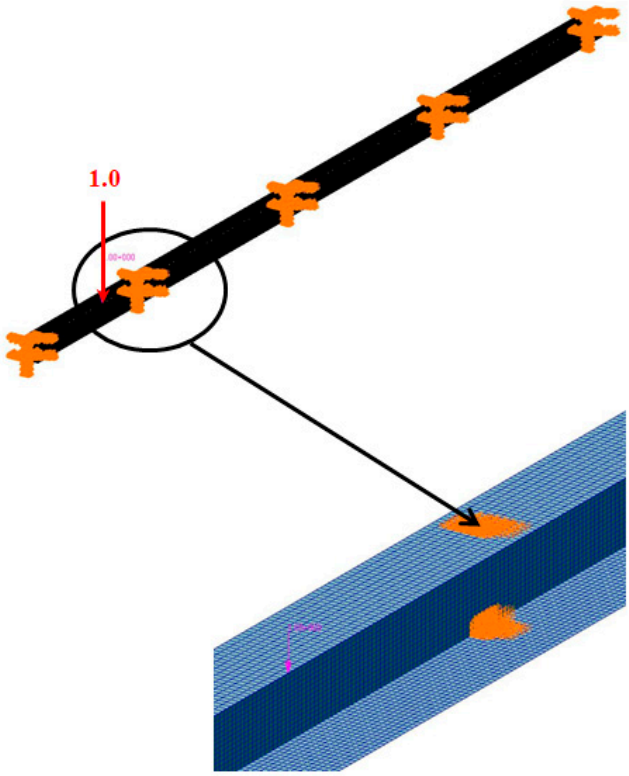

Figure 46. The dynamic model clamped at the junction of the web and flange (Case 5).

3.2. The Analysis Principle

The highest overloading capacity of the I-shaped beam is analyzed through static analysis under different clamping conditions (Case 3 and Case 4).

3.2.1. The Principle of Static Analysis

The static equilibrium equation is as follows:

$$[K]\{x\} = \{F\} \tag{7}$$

K is the total stiffness matrix, x is the displacement vector, and F is the load vector. In the static state, the resultant force and moment are zero.

$$\sum F = 0 \tag{8}$$

$$\sum M = 0 \tag{9}$$

where M is the moment about three axes of the global coordinate system.

3.2.2. The Principle of Dynamic Analysis

Please see Sections 2.2.1–2.2.3.

3.3. Results

The results presented below include those of the static and the dynamic analyses.

3.3.1. Results for Statics

In MSC.NASTRAN SOL101, it is calculated and analyzed by 100 g (g is the gravitational acceleration) overload. The displacement, stress, and strain of the workpiece in Case 3 and the reaction forces on the fixture are presented in Figures 47–50.

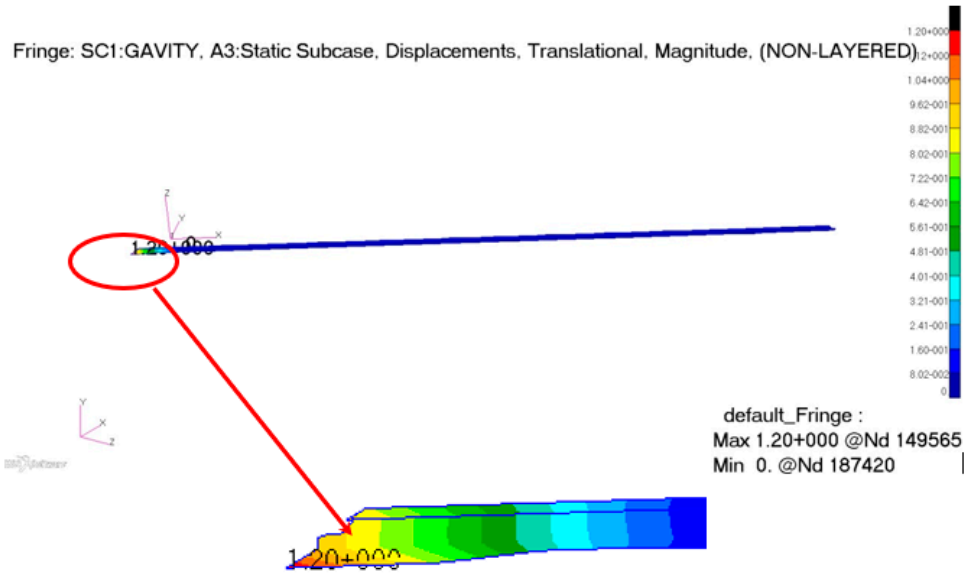

Figure 47. Displacement distribution in Case 3.

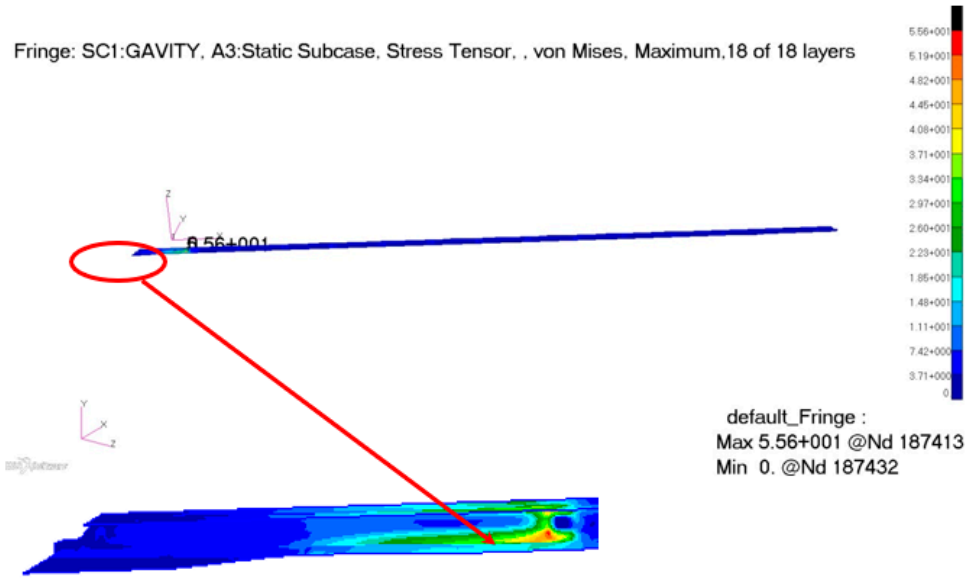

Figure 48. Stress distribution in Case 3.

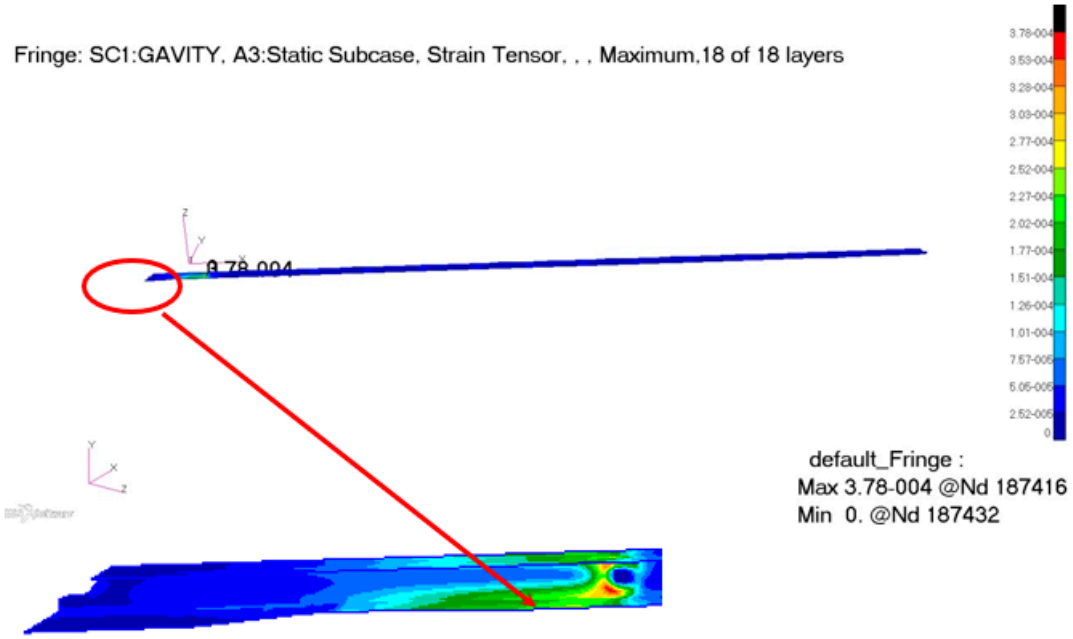

Figure 49. Strain distribution in Case 3.

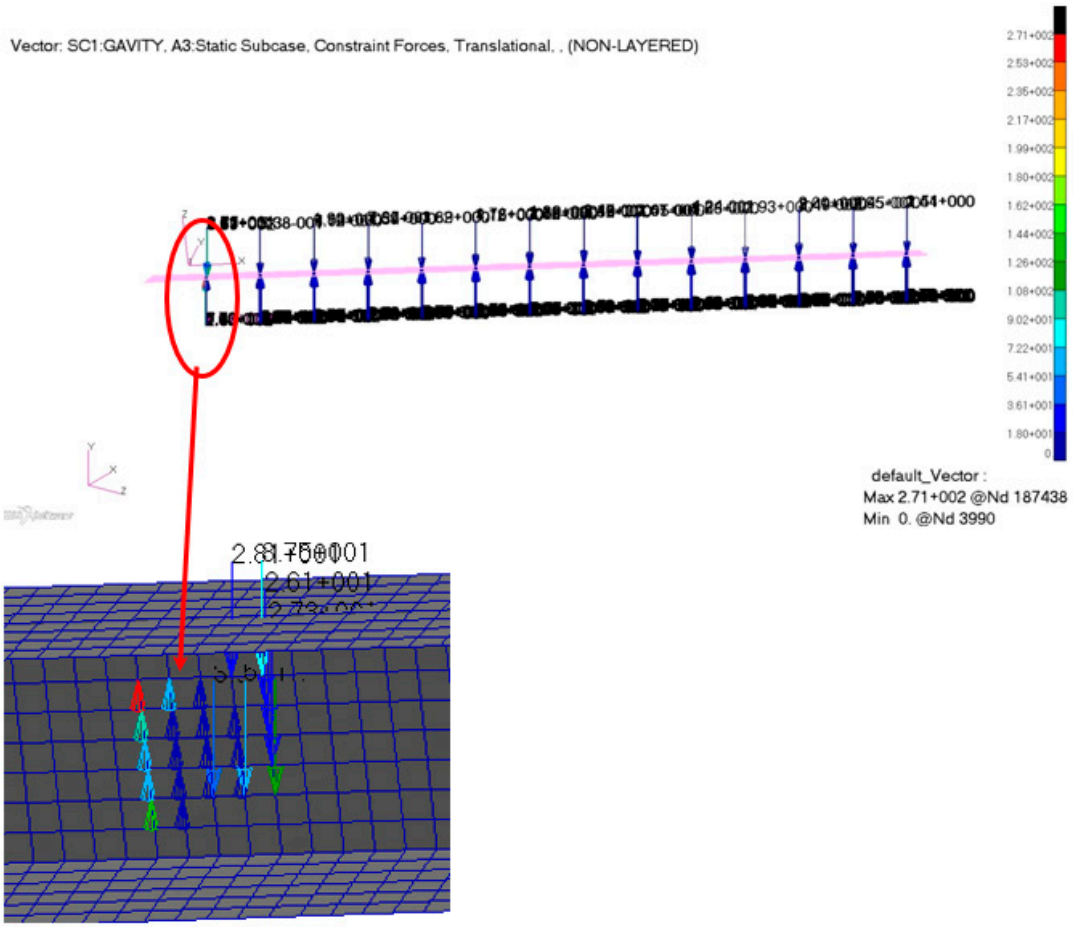

Figure 50. The reaction force on the fixture in Case 3.

In MSC.NASTRAN SOL101, it is calculated and analyzed by 100 g overload. The displacement, stress, and strain of the workpiece in Case 4 and the reaction forces on the fixture are shown in Figures 51–54.

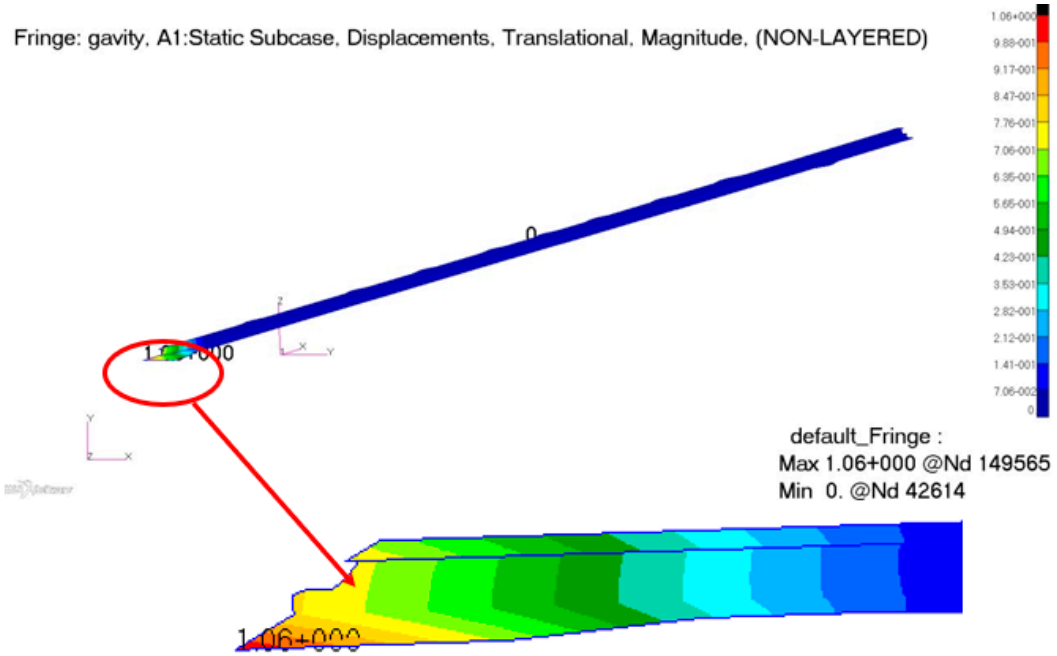

Figure 51. Displacement distribution in Case 4.

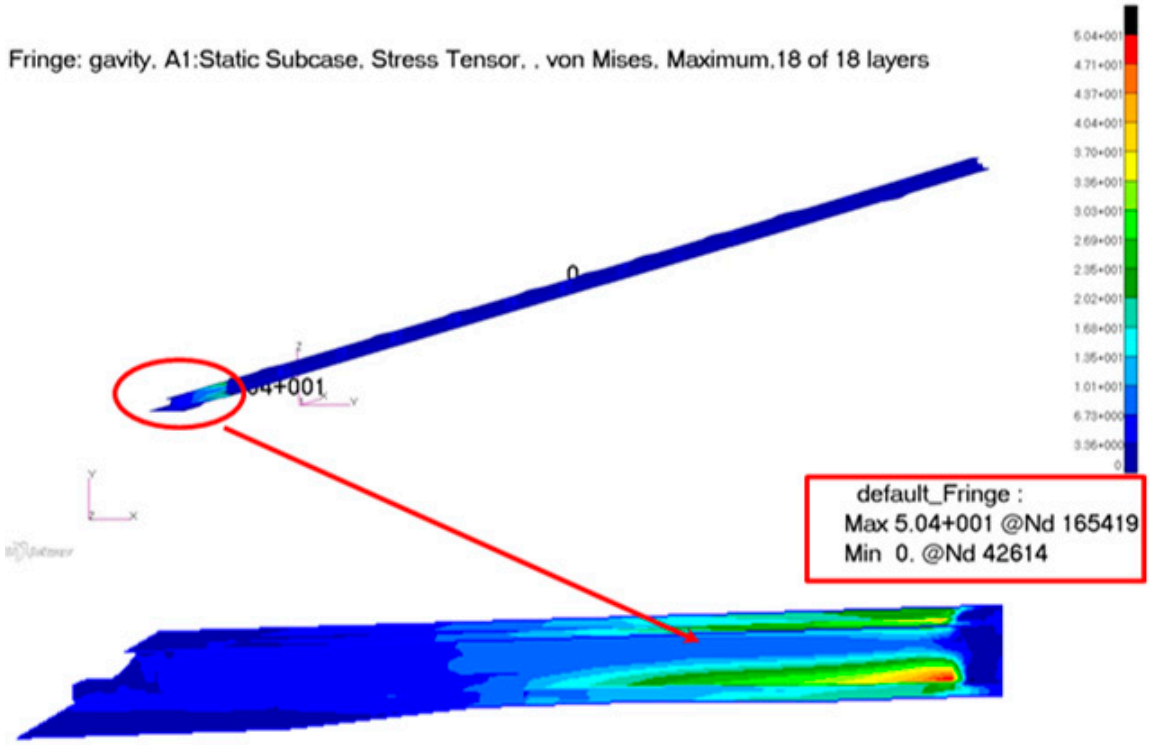

Figure 52. Stress distribution in Case 4.

From Figures 47–49 and Figures 51–53, it can be observed that the displacement, stress, and strain of the improved fixture are much lower than those of the original fixture under the maximum load. From Figures 50 and 54, it is possible to extract the reaction load of the clamp for checking the strength of the fixture. See Table 5 for a comparison.

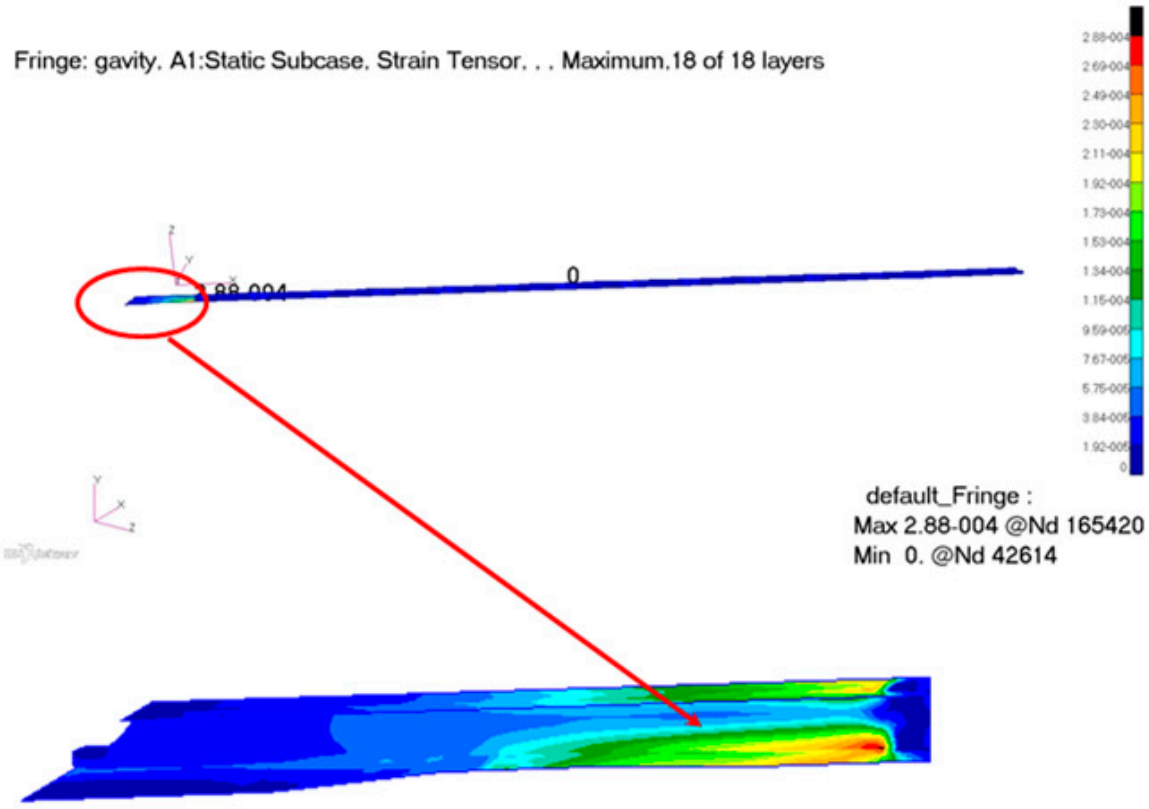

Figure 53. Strain distribution in Case 4.

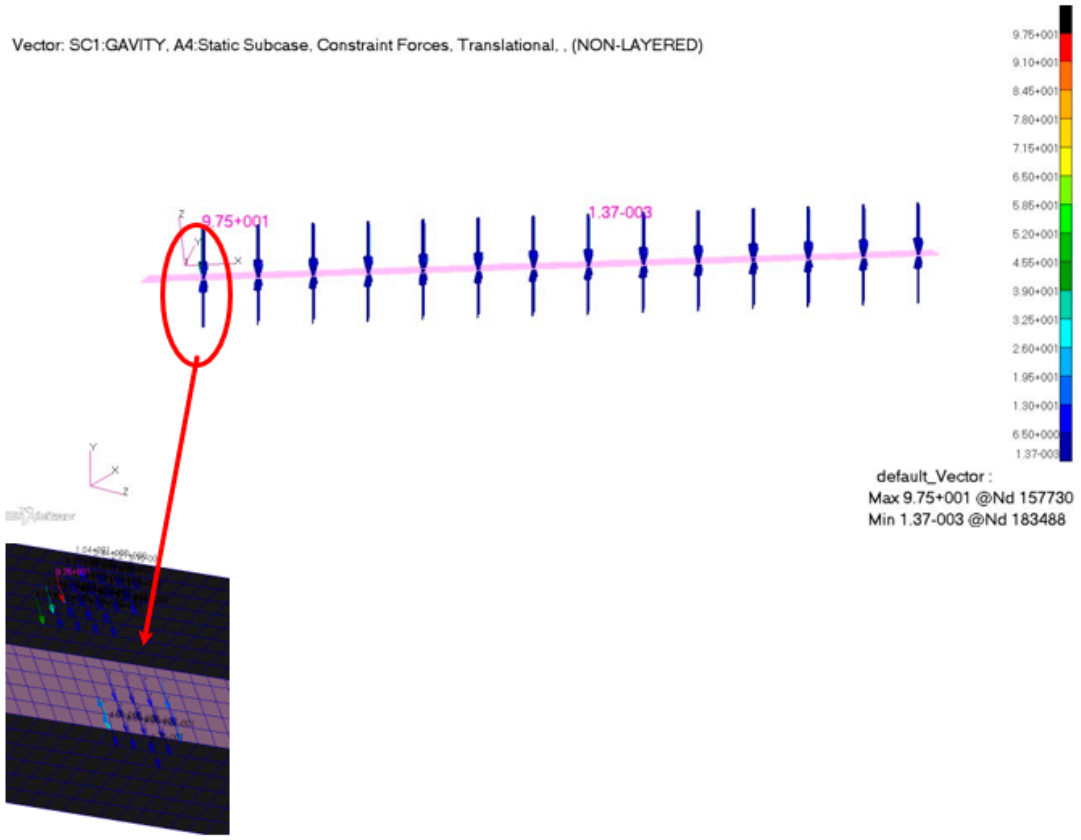

Figure 54. The reaction force on the fixture in Case 4.

Table 5. Comparison of the static results of the fixture before and after modification.

Cases	Case 3	Case 4	Difference (%)
Displacement (mm)	1.2	1.06	↓ 13.21
Stress (MPa)	55.6	50.4	↓ 10.32
Strain ($\times 10^{-6}$)	378	288	↓ 31.25

3.3.2. Dynamic Analysis Results

1. Modal analysis results

In the modal analysis of MSC.NASTRAN SOL103, Case 5's frequency and vibration modes are shown in Figures 55–64.

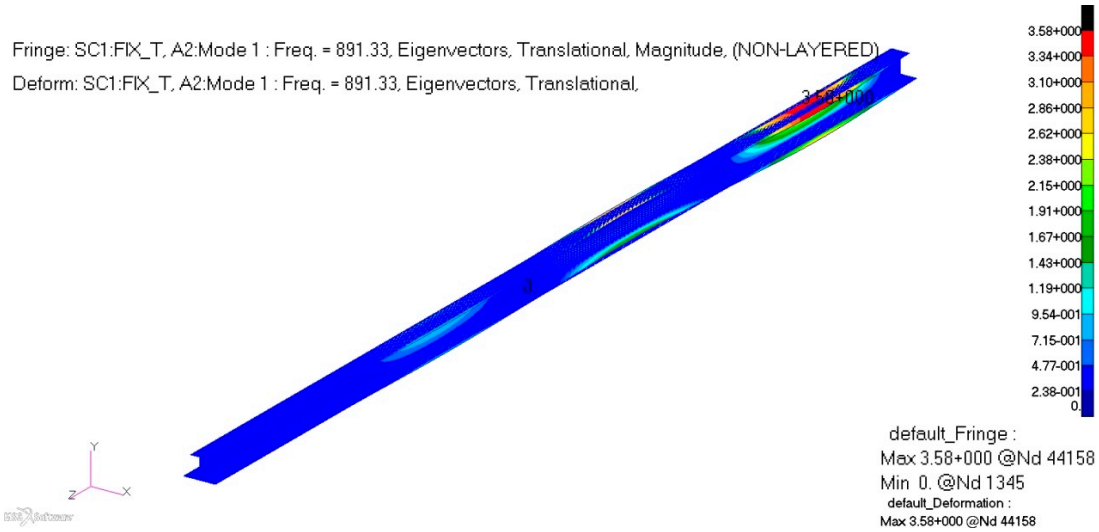

Figure 55. 1st mode.

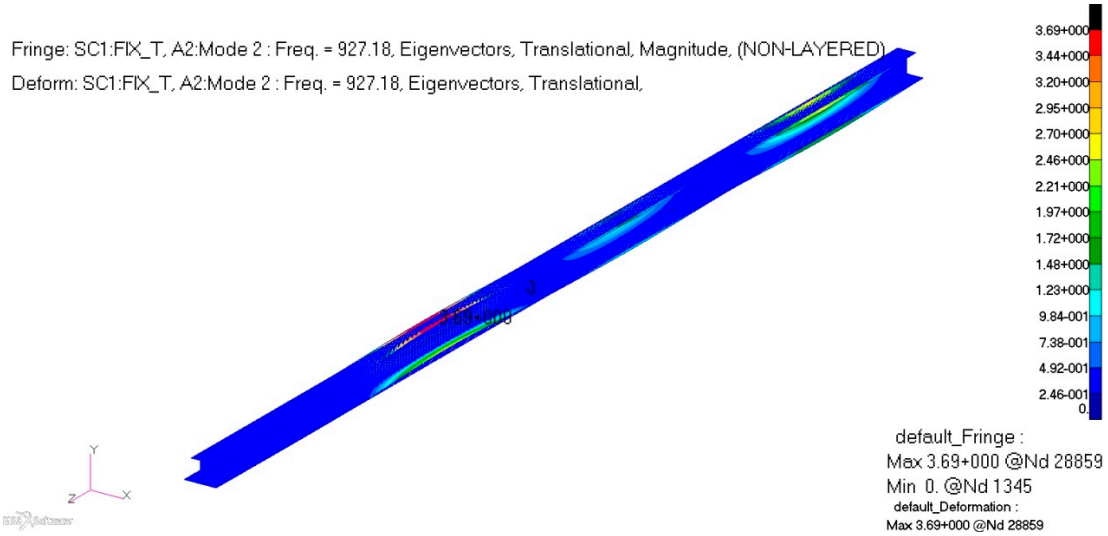

Figure 56. 2nd mode.

From Figures 55–64, Case 1 and Case 5 have the same natural mode shapes, and the model of Case 5 has a higher frequency than that of Case 1. The lowest frequency of Case 1 is 546.63 Hz and that of Case 5 is 891.33 Hz, which are much higher than the natural frequency of 83.33 Hz of the cutting tool. See Table 6 for a comparison of the natural frequencies.

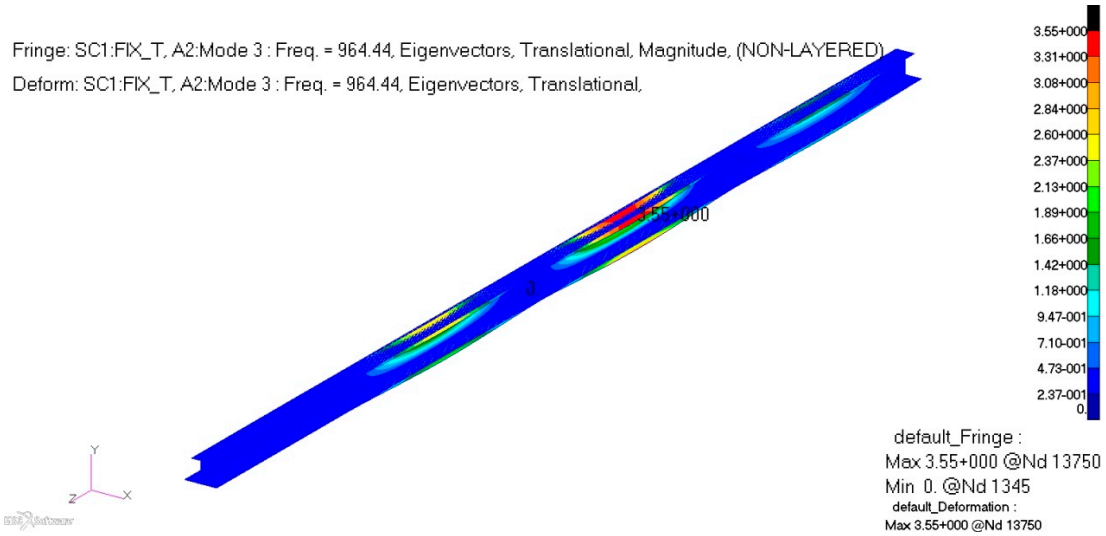

Figure 57. 3rd mode.

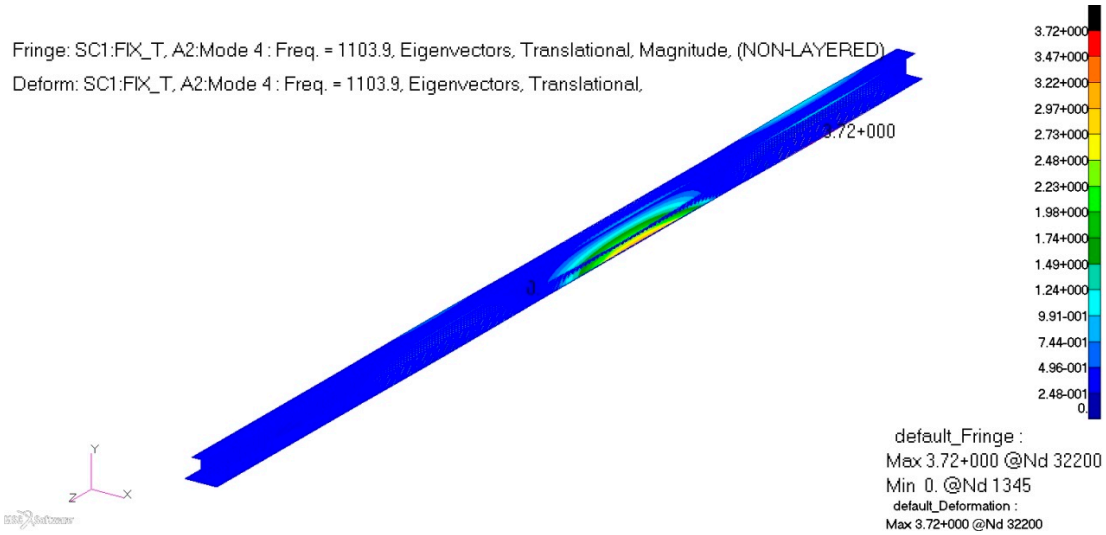

Figure 58. 4th mode.

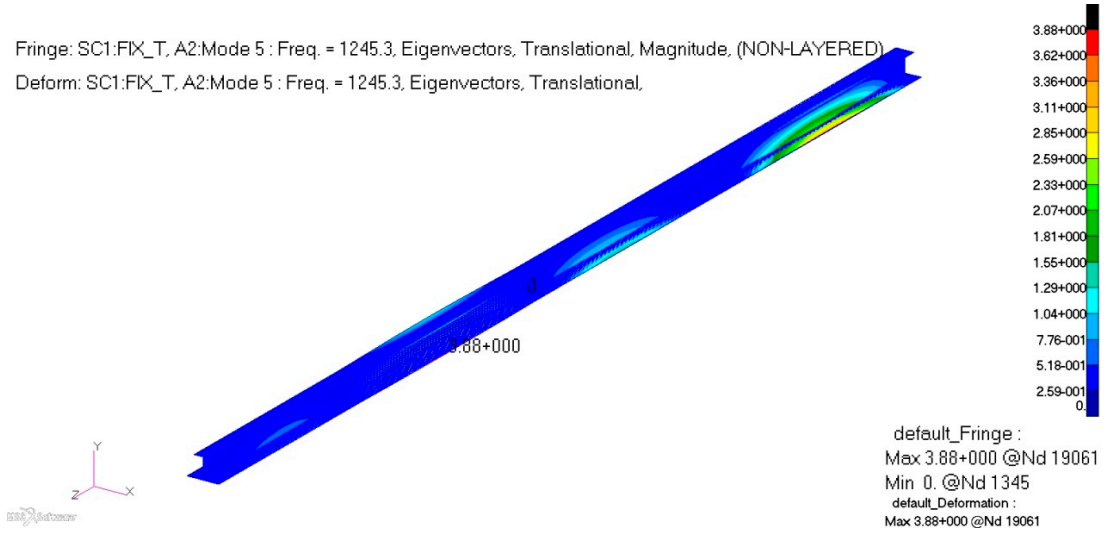

Figure 59. 5th mode.

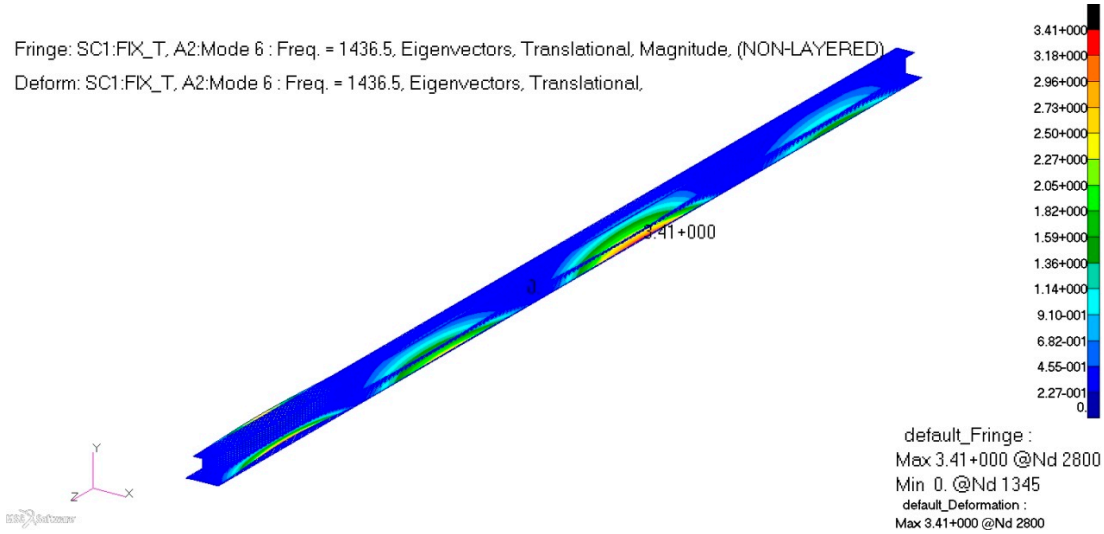

Figure 60. 6th mode.

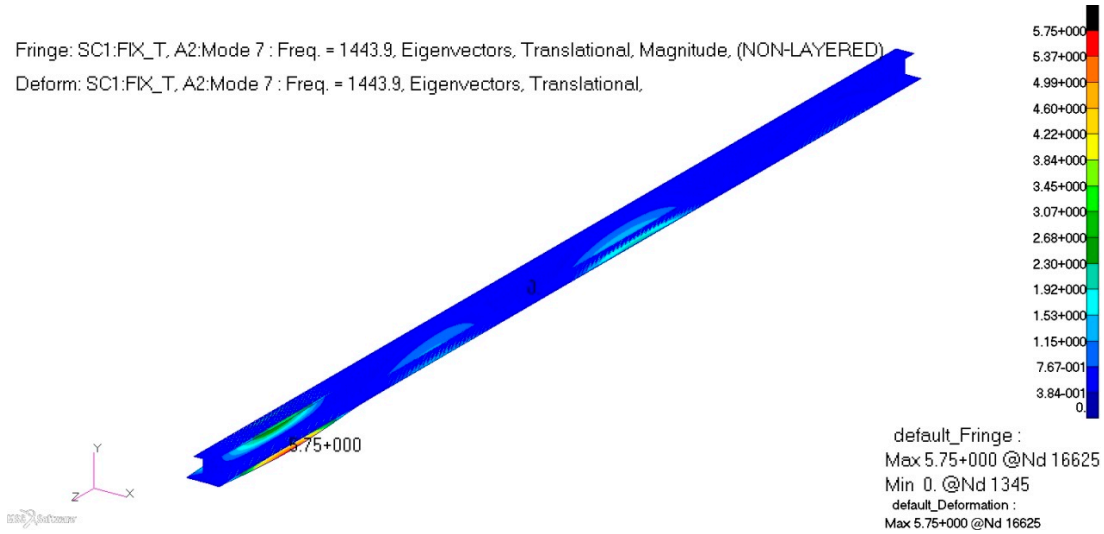

Figure 61. 7th mode.

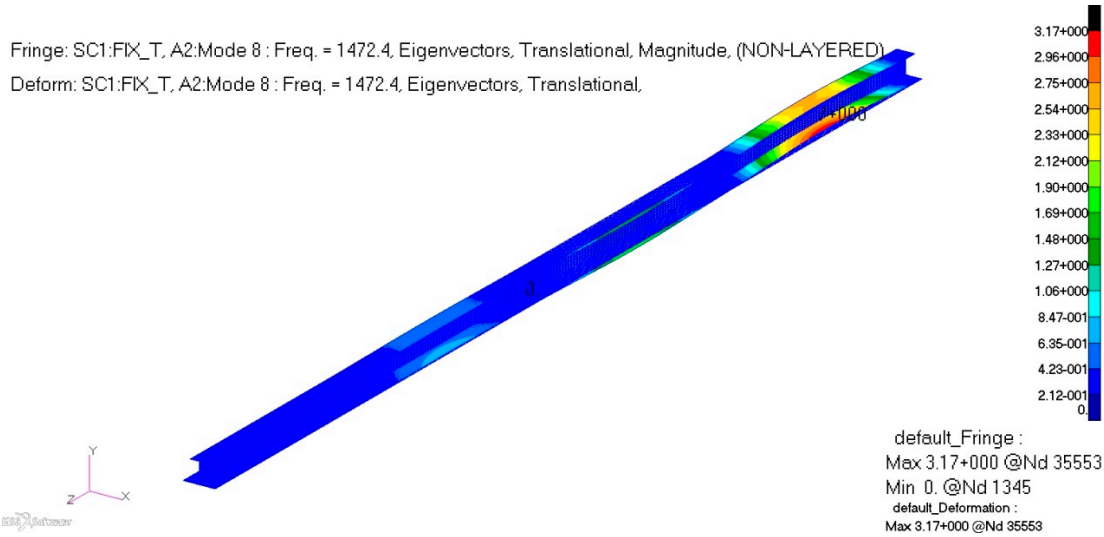

Figure 62. 8th mode.

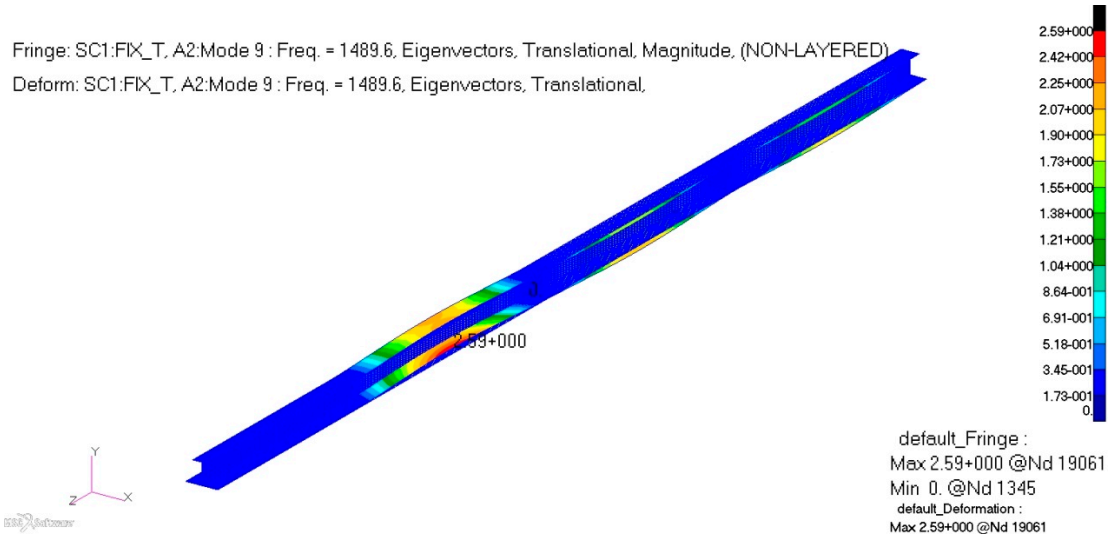

Figure 63. 9th mode.

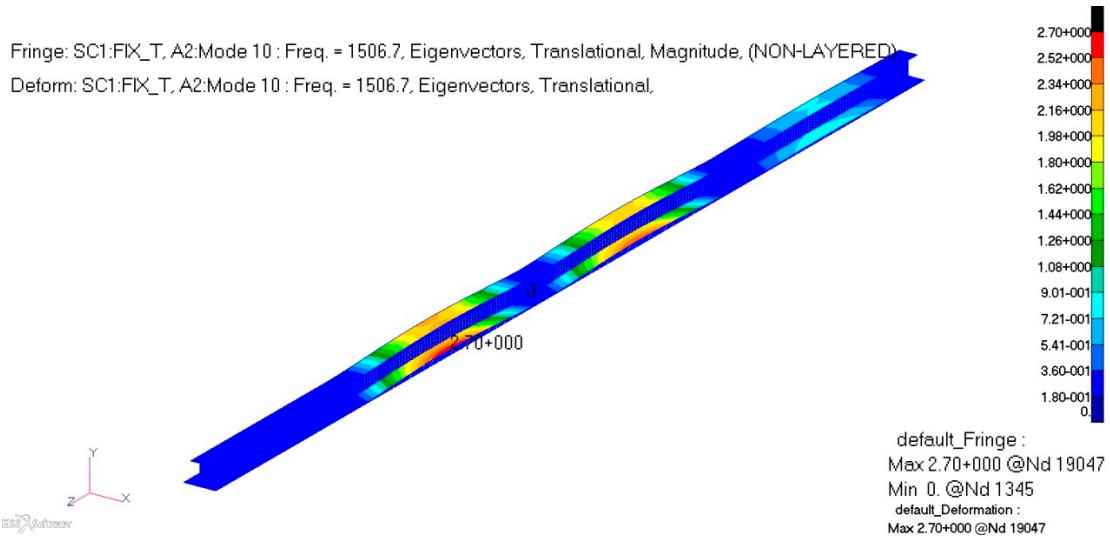

Figure 64. 10th mode.

Table 6. Comparison of the natural frequencies in Case 1 and Case 5.

Cases	Case 1 (Hz)	Case 5 (Hz)	Difference (%)
1st mode	546.63	891.33	↑ 63.05910762
2nd mode	628.59	927.18	↑ 47.50155109
3rd mode	704.81	964.44	↑ 36.83687802
4th mode	733.71	1103.9	↑ 50.45453926
5th mode	794.12	1245.3	↑ 56.81509092
6th mode	811.84	1436.5	↑ 76.94373276
7th mode	942.03	1443.9	↑ 53.2753734
8th mode	1073.7	1472.4	↑ 37.13327745
9th mode	1214.4	1489.6	↑ 22.66139657
10th mode	1319.9	1506.7	↑ 14.15258732

2. Results of Frequency Response Analysis

An equal 1-unit impact sine load is applied to the upper flange of the I-shaped beam with the improved fixture. MSC.NASTRAN SOL111 is used to solve this dynamic model (See Figure 46). The results are shown in Figures 65–70.

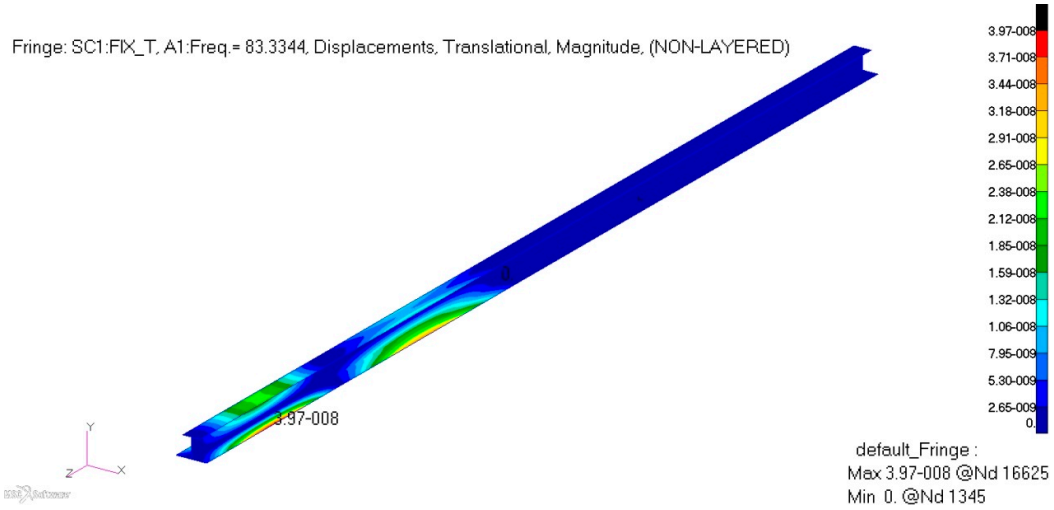

Figure 65. Vibration displacement of the I-shaped beam in Case 5 (f = 83.3344 Hz).

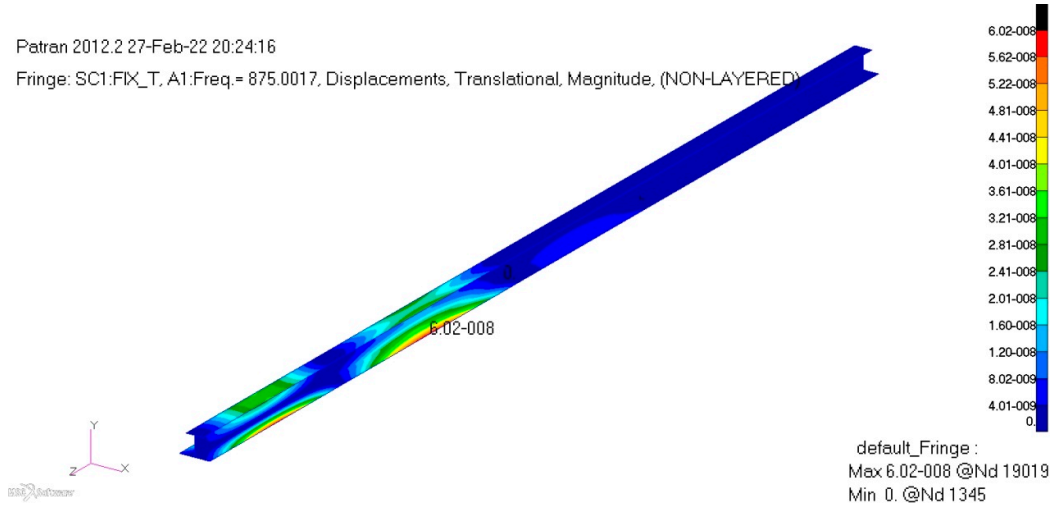

Figure 66. Vibration displacement of the I-shaped beam in Case 5 (f = 875.00174 Hz).

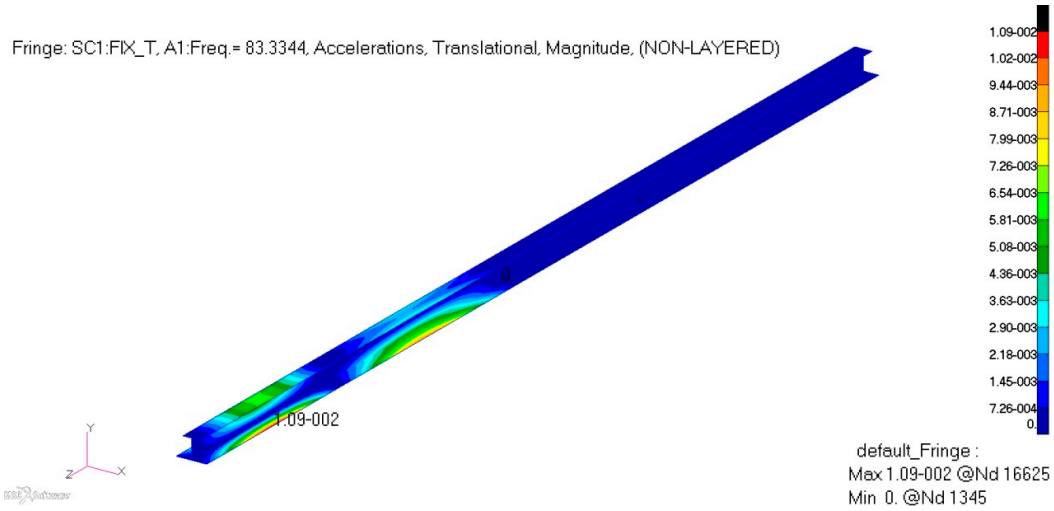

Figure 67. Vibration acceleration of the I-shaped beam in Case 5 (f = 83.3344 Hz).

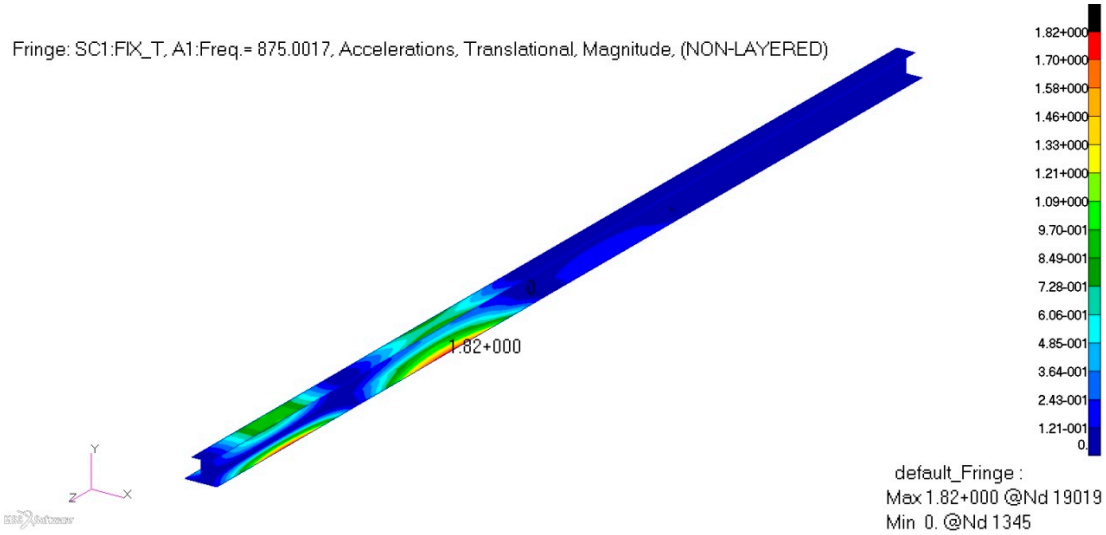

Figure 68. Vibration acceleration of the I-shaped beam in Case 5 (f = 875.0017 Hz).

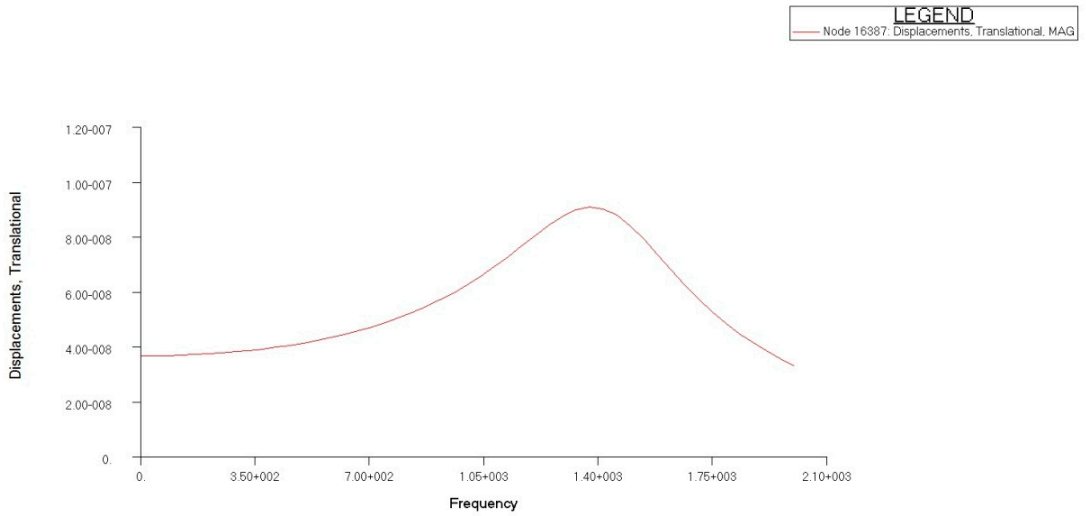

Figure 69. Typical node displacement with frequency in Case 5.

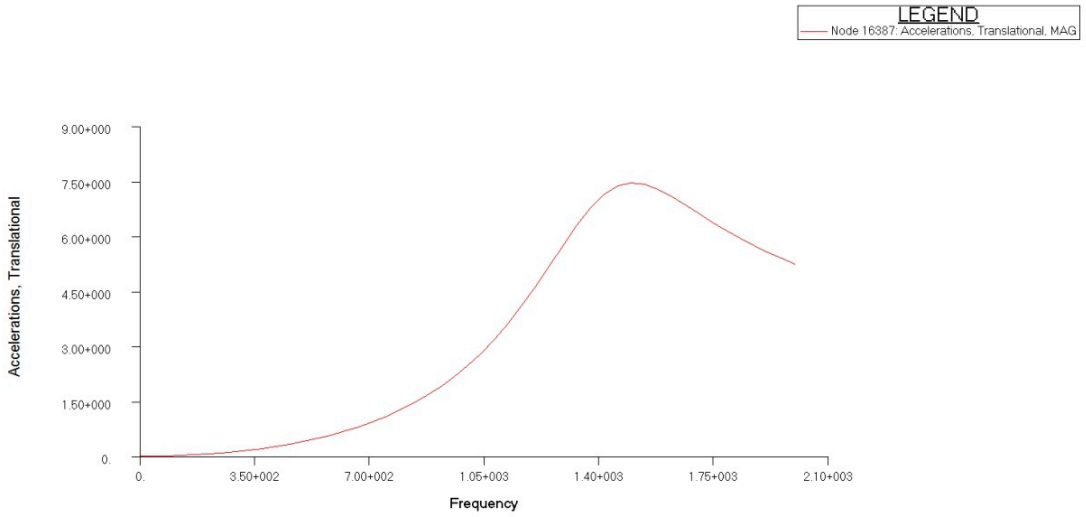

Figure 70. Typical node acceleration with frequency in Case 5.

According to the dynamic responses of Case 1 and Case 5, the vibration displacement and acceleration of Case 1 are higher than those of Case 5 at the natural vibration frequency of 83.33 Hz. The peak values of the vibration displacement and vibration acceleration of Case 1 occur at about 870 Hz, while those of the vibration displacement and vibration acceleration of Case 5 occur at about 1500 Hz. The max vibration displacement and vibration acceleration of Case 1 are much higher than those of Case 5, whose displacement is reduced to 1/8 and acceleration is reduced to 1/3.

3. Random Response Analysis Results

After frequency response analysis of Case 5, white noise is implemented to analyze the random response. Figures 71 and 72 show the results.

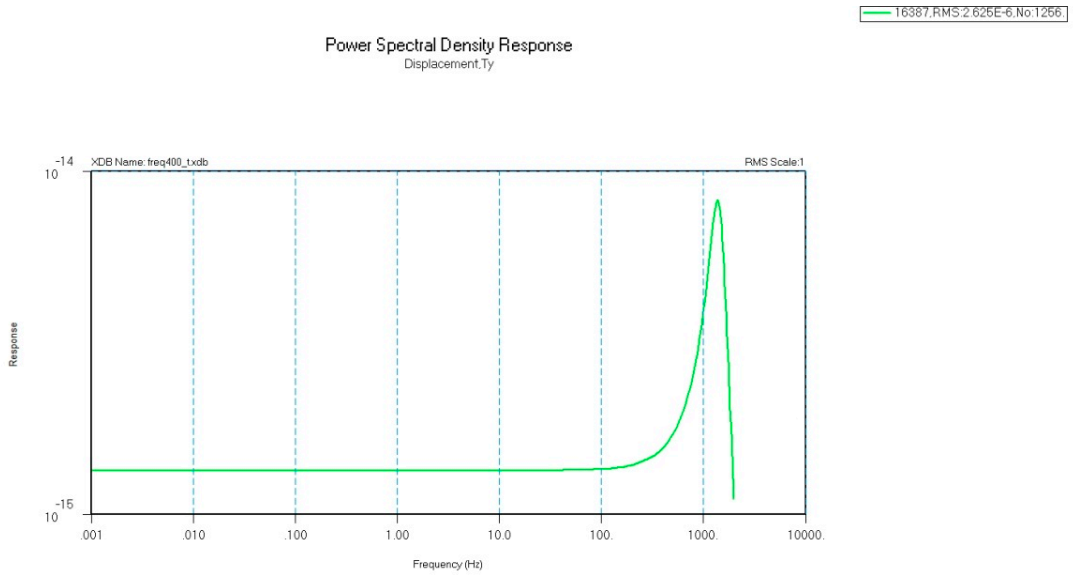

Figure 71. PSD response of *y*-axis displacement of the typical node in Case 5.

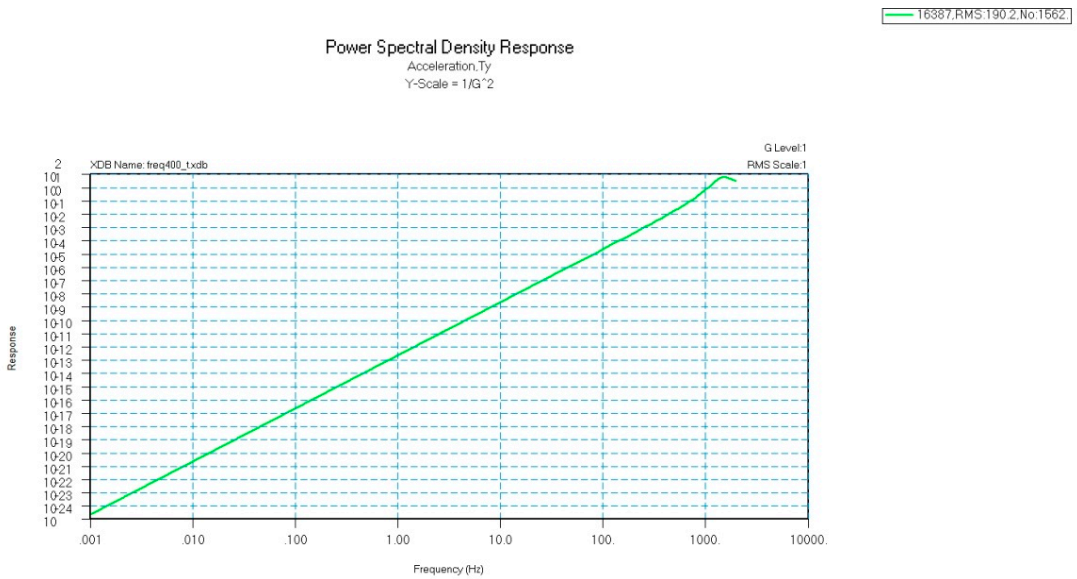

Figure 72. PSD response of *y*-axis acceleration of the typical node in Case 5.

According to the 2000 Hz frequency's sweep, the vibration displacement and acceleration's PSD of Case 1 at about 870 Hz are much larger than those of Case 5 at about 1500 Hz. The displacement of Case 5 is two orders of magnitude smaller than that of Case 1. The acceleration of Case 5 is one order of magnitude smaller than that of Case 1.

3.4. Discussion

According to the static and dynamic analysis of the above two different clamping patterns, the improved "L" clamping mode of Case 4 can reduce the bending moment produced by the cutting force of the tool. In particular, the cutting load can be directly transmitted to the fixed upper and lower junctions, so that the load transfer is simple and direct.

According to the static analysis, the displacement, stress, and strain of the improved fixture decreased greatly under 100 g overload, which are decreased by 13.21%, 10.32%, and 31.25%, respectively. The static simulation can serve to extract the load at the fixture and check the strength of the fixture in the future.

From the modal analysis, the improved fixture increases the natural frequency of the structure (most of the frequencies increased by 50%). From the frequency response analysis, the improved fixture significantly reduces the vibration displacement by 7/8 and the acceleration by 2/3 when the workpiece is machined. The improved fixture reduces the peak PSDs of the displacement and acceleration of the workpiece by two and one orders of magnitude, respectively.

According to the model analyses of the new and old clamping modes and positions, whether static or dynamic analysis, the load-bearing capacity and vibration reduction effect of the new fixture are better than those of the old one.

4. Conclusions

In this paper, the influence of changes in the clamping approach, including the distance and clamping mode of the fixture, on the vibration of the workpiece is discussed.

Through the contrast analysis of three kinds of clamping distances, we choose the optimal clamping distance of 0.4 m. The simulation analysis also shows that shortening the clamping distance does not significantly reduce the vibration of the workpiece, and therefore, one should actively seek other ways to reduce the vibration of the workpiece processing, such as not changing the clamping distance but changing the clamping mode and position.

According to the static and dynamic analyses of the models of new and old clamping modes and positions, we also select the new fixture as the final design.

The work and results in this paper support the fixture proofing and also lay a foundation for the smooth production of the beam machining. The results presented in this paper may be relevant to the machining of similar thin-walled elongated beams.

Author Contributions: Conceptualization, J.Q. and C.S.; methodology, J.T.; software, J.Q.; validation, Y.G. and H.R.; formal analysis, J.Q.; investigation, J.Q.; resources, J.T.; data curation, H.R.; writing—original draft preparation, J.Q.; writing—review and editing, J.Q.; visualization, H.R.; supervision, J.Q.; project administration, C.S. All authors have read and agreed to the published version of the manuscript.

Funding: This research received no external funding.

Data Availability Statement: Not applicable.

Conflicts of Interest: The authors declare no conflict of interest.

References

1. Shenoy, P.; Nithesh, N.; Shettar, M.; Abbas, W. Design and Analysis of Split Fixture for Gear Hobbing Machine. *MATEC Web Conf.* **2018**, *144*, 8–15. [CrossRef]
2. Olabanji, O.; Mpofu, K.; Battaïa, O. Design, simulation and experimental investigation of a novel reconfigurable assembly fixture for press brakes. *Int. J. Adv. Manuf. Technol.* **2016**, *82*, 663–679. [CrossRef]
3. Amaral, N.; Rencis, J.J.; Rong, Y. Development of a finite element analysis tool for fixture design integrity verification and optimisation. *Int. J. Adv. Manuf. Technol.* **2005**, *25*, 409–419. [CrossRef]
4. Khan, A.A.; Moeenuddin, G.; Kazim, A.H.; Kamran, M.S.; Asim, M. An integrated system for process-fixture layout design optimisation for cubical parts. *South Afr. J. Ind. Eng.* **2019**, *30*, 83–99. [CrossRef]
5. Xing, Y. Fixture Layout Design of Sheet Metal Parts Based on Global Optimization Algorithms. *J. Manuf. Sci. Eng.* **2017**, *139*, 101004. [CrossRef]

6. Xing, Y.; Hu, M.; Zeng, H.; Wang, Y. Fixture layout optimisation based on a non-domination sorting social radiation algorithm for auto-body parts. *Int. J. Prod. Res.* **2015**, *53*, 3475–3490. [CrossRef]
7. Xiong, L.; Molfino, R.; Zoppi, M. Fixture layout optimization for flexible aerospace parts based on self-reconfigurable swarm intelligent fixture system. *Int. J. Adv. Manuf. Technol.* **2013**, *66*, 1305–1313. [CrossRef]
8. Illidge, A.; Bright, G. An Automated Flexible Fixture System for Mass Customisation. *South Afr. J. Ind. Eng.* **2018**, *29*, 21–34+14.
9. Ramnath, B.V.; Elanchezhian, C.; Rajesh, S.; Prakash, S.J.; Kumaar, B.M.; Rajeshkannan, K. Design and Development of Milling Fixture for Friction Stir Welding. *Mater. Today Proc.* **2018**, *5*, 1832–1838. [CrossRef]
10. Liang, Z.; Zhao, C.; Zhou, H.; Zhou, Y. Investigation on fixture design and precision stability of new-type double collect chuck for machining of long ladder shaft gear. *J. Mech. Sci. Technol.* **2019**, *33*, 323–332. [CrossRef]
11. Yu, K.; Wang, S.; Wang, Y.; Yang, Z. A flexible fixture design method research for similar automotive body parts of different automobiles. *Adv. Mech. Eng.* **2018**, *10*, 1687814018761272. [CrossRef]
12. Zhang, F.P.; Wu, D.; Zhang, T.H.; Yan, Y.; Butt, S.I. Knowledge component-based intelligent method for fixture design. *Int. J. Adv. Manuf. Technol.* **2018**, *94*, 4139–4157. [CrossRef]
13. Denkena, B.; Bergmann, B.; Kiesner, J. Increasing the Measuring Accuracy of a Sensory Swing Clamp by Multi-Sensor Evaluation. *J. Manuf. Sci. Eng.* **2019**, *141*, 111007. [CrossRef]
14. MSC. SOFTWARE Corporation. MSC. Nastran Preference Guide Vol. 1, Structural Analysis. Santa Ana CA: [s. n.]. 2010. Available online: https://www.scribd.com/document/74993284/Nastran-Preference-Guide-Volume-1-Structural-Analysis (accessed on 18 August 2023).
15. Qiu, J.; Lian, W.; Rao, H.; Wang, C.; Luo, T.; Tang, J. Localization of Vibration Weak Position of Composites Based on Weighted Modal Strain Energy Summation. *J. Compos. Sci.* **2022**, *6*, 324. [CrossRef]